Naturwissenschaften (2004) 91:101–122
DOI 10.1007/s00114-004-0502-3

REVIEW

Fritz-Olaf Lehmann

The mechanisms of lift enhancement in insect flight

Published online: 4 March 2004

Abstract Recent studies have revealed a diverse array of fluid dynamic phenomena that enhance lift production during flapping insect flight. Physical and analytical models of oscillating wings have demonstrated that a prominent vortex attached to the wing's leading edge augments lift production throughout the translational parts of the stroke cycle, whereas aerodynamic circulation due to wing rotation, and possibly momentum transfer due to a recovery of wake energy, may increase lift at the end of each half stroke. Compared to the predictions derived from conventional steady-state aerodynamic theory, these unsteady aerodynamic mechanisms may account for the majority of total lift produced by a flying insect. In addition to contributing to the lift required to keep the insect aloft, manipulation of the translational and rotational aerodynamic mechanisms may provide a potent means by which a flying animal can modulate direction and magnitude of flight forces for manoeuvring flight control and steering behaviour. The attainment of flight, including the ability to control aerodynamic forces by the neuromuscular system, is a classic paradigm of the remarkable adaptability that flying insects have for utilising the principles of unsteady fluid dynamics. Applying these principles to biology broadens our understanding of how the diverse patterns of wing motion displayed by the different insect species have been developed throughout their long evolutionary history.

Introduction

Over the last of couple of years there has been tremendous progress in understanding the locomotor system of flying insects. New concepts have tackled long-standing mysteries of aerodynamic force production in flapping wings that has drawn the attention of both biologists and engineers in this field. Some of this progress relies on advancements in technology such as robotics and computational fluid dynamics that are essential tools for understanding the basis of aerodynamic force production (Kamakoti et al. 2000, 2002; Lan 1979; Liu 2002; Liu et al. 1998; Ramamurti and Sandberg 2001; Sun and Hamdani 2001; Sun and Tang 2002; Sunada 1993; Walker 2002b; Walker and Westneat 2000; Z.J. Wang et al. 2003). Affordable high-speed video systems allow biologists to routinely study wing motion in flying animals in order to explore the repertoire of wing kinematics in living animals, and physical models such as dynamically-scaled robotic wings demonstrate unconventional aerodynamic phenomena based on nonsteady (unsteady) aerodynamic mechanisms (Bennett 1966; Dickinson et al. 1999; Ellington et al. 1996; Maxworthy 1979; Spedding and Maxworthy 1986; Sunada et al. 2002). The development of man-made small flying micro-air-vehicles with the size of a large insect currently helps biologists and engineers to understand the basis of flight force production on a more elaborate and integrative level of investigation (Ellington 1999; Norberg 2002; Schenato et al. 2001; Shyy et al. 1999; Zbikowski 2002). Such integrative studies are of fundamental importance for understanding the general biomechanics of locomotor systems in animals, including sensory processing and neuromuscular control, and broaden our comprehension of how a locomotor system such as the insect flight motor has been shaped by an evolutionary history of more than 300 million years.

Insects are masters of flight agility and manoeuvrability when hunting for prey, circling around flowers or when landing upside down on the undersurface of a leaf (Alexander 1986; Azuma and Watanabe 1988; Crompton et al. 2003; Dudley 2002; Land and Collett 1974; Srygley and Dudley 1993; Taylor 2001; Wagner 1985; H. Wang et al. 2003; Wehrhahn et al. 1982; Zeil 1983). Flight manoeuvres result from a process in which an insect

F.-O. Lehmann (✉)
BioFuture Research Group, Department of Neurobiology,
University of Ulm,
Albert-Einstein-Allee 11, 89081 Ulm, Germany
e-mail: fritz.lehmann@biologie.uni-ulm.de
Tel.: +49-731-5023122
Fax: +49-731-5022629

converts elaborate sensory feedback or intrinsic commands into changes in aerodynamic forces produced by the flapping wings (Alexander 1982; Egelhaaf 1989; Flick et al. 2001; Fry et al. 2003; Götz 1968, 1983; Götz et al. 1979; Hausen and Wehrhahn 1990; Heide 1975, 1983; Heide and Götz 1996; Heisenberg and Wolf 1988, 1993). The wings leave behind a *wake* in which any change in force production is imprinted because forces require an opposite change in momentum of the surrounding fluid. Thus the wake is the last component visible in the cascade ranging from neural control to flight muscle activation, structural mechanics of the wing hinge, and aerodynamic mechanisms. One of the major goals in insect flight research is to understand the interface between changes in wake structure, and spatial and temporal alterations in aerodynamic forces resulting from the complex acceleration pattern of the fluid. Consequently, in order to dissect the basis of aerodynamic force production in insects, it requires an approach from two different directions: first, by determining the time course of aerodynamic force production within each stroke cycle and, second, by quantifying both flow separation at the wing and the structure of the resulting wake in space and time.

Traditional approaches to studying flight force production in birds, bats, or insects were often dominated by 'quasi-steady' models in which the time variant properties of aerodynamic force coefficients were ignored (Dudley and Ellington 1990b; Ellington 1975, 1984e; Nachtigall 1977; Newman et al. 1977; Norberg 1975a, 1975b, 1976; Okamoto et al. 1996; Wakeling and Ellington 1997b; Weis-Fogh 1972, 1973; Zanker and Götz 1990). Most of the mystery inherent in insect flight force production is attributable to this approach because these models cannot account for unsteady aerodynamic effects such as leading-edge vorticity or the Wagner effect (Wagner 1925). Moreover, many researchers limited their analysis to two-dimensional conditions in which the wing is modelled as a series of chordwise wing blade elements that produce aerodynamic forces without flow interaction between adjacent wing elements. Two-dimensional experiments relevant to flapping flight were done by Maxworthy (1979), Savage et al. (1979), Spedding and Maxworthy (1986), Dickinson and Götz (1993) and Dickinson (1994).

In real three-dimensional wings, however, there is a spanwise interaction of fluid modifying the flow pattern that the wing is generating while it travels through the fluid. Consequently, our problems in understanding force production in flapping wings in the past stemmed from two separate simplifications: the time-averaged force coefficients typically derived by testing the wing in a wind tunnel, and the assumption that the flow around the wing can be described as a result of flow in multiple independently acting spanwise wing elements. The recent progress in experimental methods on robotic wings and two-dimensional computation of the details of vorticity generation in the flow around wings, including its relation to flight forces, has led to a new depiction of aerodynamic mechanisms in flight (Dickinson et al. 1999; Ellington et al. 1996; Wang 2000a, 2000b). In particular, the development in our understanding of unsteady aerodynamic mechanisms currently allows us to gain a deeper insight into how flapping wings produce lift and complex three-dimensional wakes which, in turn, broadens our comprehension of how the variety of different kinematic patterns found in flying insects might have evolved.

The quasi-steady approach

Wings produce lift by accelerating a fluid volume in a vertical direction. The simplest view of flight is thus to consider the flapping wings as a device (actuator disc) that pushes air downwards at a certain rate (Ellington 1984d). This approach is termed the Rankine-Froude momentum theory or 'helicopter theory', considering the wake below the moving wings as a fluid jet with a uniform velocity distribution (von Mises 1959). The amount of force that a wing produces is equal to the change in fluid momentum per unit time (momentum rate) and can be derived simply by the product between the mass of the fluid volume times its acceleration. However, the momentum jet theory considers insect flight on a superficial level and ignores any variations in wing size, wing morphology, kinematics and lift-producing mechanisms.

To predict aerodynamic forces from the motion of wings in more detail, many researchers have estimated lift forces in flying animals using a more elaborated expression of Newton's view on force production (flight force is proportional to wing velocity squared) valid at high Reynolds numbers. The approach can be simplified by considering the fluid flow around an infinitesimal chordwise wing element (wing segment) of a wing with infinite length (span) to be *two-dimensional*, ignoring *three-dimensional* effects such as wing-tip vorticity and spanwise flow. Lift L per unit wing span is defined as a force acting perpendicular to the incident flow and given by

$$L_c = \frac{1}{2}\rho C_L(\alpha_{eff})u^2 c dr \quad (1)$$

in which ρ is the density of the fluid, u is local flow velocity, c is wing chord and C_L the lift coefficient. The second force component on the wing is drag D that acts parallel to the incident flow and is given by

$$D_c = \frac{1}{2}\rho C_D(\alpha_{eff})u^2 c dr \quad (2)$$

in which C_D is the drag coefficient. The dimensionless coefficients C_L and C_D determine how much force a wing produces while moving through the fluid at a certain speed and at a certain effective angle of attack α_{eff} (Fig. 1). Since, in most cases, the effective angle of attack can not be derived simply from wing motion, we have to consider the wing's angle of attack in greater detail. The *geometrical* or *morphological* angle of attack α_g refers to the angle between a wing segment and a geometrically defined reference line typically the direction of wing motion (Fig. 1). In contrast, the *effective* or

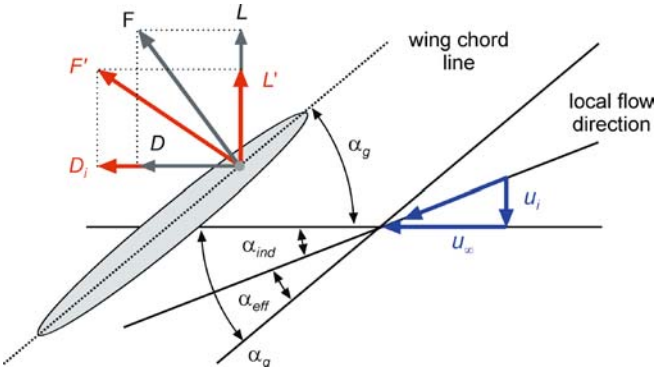

Fig. 1 Schematic of forces and flow directions in a translating chordwise wing element. Forces assuming two-dimensional flow conditions are shown by *grey vectors*. Forces influenced by the generation of wing-tip vortex in a real three-dimensional aerofoil are *plotted in red*. Induced drag tilts the total force vector slightly backwards which attenuates aerodynamic lift production. *Blue vectors* indicate the direction and magnitude of flow that acts on the wing. The local flow conditions given by the effective angle of attack and the local fluid velocity depend on the wing's geometrical angle of attack, induced velocity and the free stream velocity of the fluid. u_i = induced velocity due to the downward acceleration of fluid; u_∞= free stream velocity (relative wind) towards the wing surface due to wing motion; α_g= geometrical angle of attack of the wing; α_{ind}= angle of the induced flow with respect to the wing's own motion; α_{eff} = effective angle of attack; F= total force and L= lift acting on the wing assuming two-dimensional flow conditions, respectively; D= wing drag which is equal to the sum of pressure drag and skin friction; F'= total force and L'= lift in a three-dimensional wing, respectively, and D_i= induced drag due to tip vortex

aerodynamic angle of attack α_{eff} results from the vector sum between the incident velocity of the oncoming fluid u_∞ and the induced flow u_i generated by the moving wings termed *downwash*. Without induced flow, geometrical and effective angle of attack are equal. Because of downwash, the wing's effective angle of attack yields (von Mises 1959):

$$\alpha_{eff} = \alpha_g - \tan^{-1}\left(\frac{u_\infty}{u_i}\right) \quad (3)$$

Lift and drag forces are the vector components of the total force vector that acts on the wing (Fig. 1). According to thin aerofoil theory, at high Reynolds number the aerodynamic force vector is dominated by pressure around the wing (pressure lift and drag) and thus orientated perpendicular to the centre line of the wing profile (Fung 1993). Consequently, when moving through the fluid, a wing generates an aerodynamic force per unit wing span F_c, which is given by

$$F_c = \left(L_c^2 + D_c^2\right)^{0.5} \quad (4)$$

In a real three-dimensional wing moving in a real fluid, however, pressure drag ($C_{D,\,p}$) is only one component of total wing drag that also involves *induced drag* ($C_{D,\,i}$) and *skin friction* ($C_{D,sf}$). Induced drag results as a consequence of lift production on (real) aerofoils with finite wing length and is ignored in a two-dimensional approach. Induced drag adds to pressure drag and tilts the force vector slightly backwards in the direction of the moving fluid (Fig. 1). The significance of induced drag for unsteady aerodynamic mechanisms is discussed in more detail when considering the mechanisms of vortex stabilisation on insect wings later in this review. Skin friction is important in most insects flying at intermediate Reynolds numbers, and results from the viscous forces in the fluid due to shear stress. Skin friction significantly attenuates the production of pressure forces caused by the fluid acceleration around the wing and quickly increases with increasing pressure gradients and surface roughness, and with decreasing Reynolds number (Thom and Swart 1940). In thin aerofoils such as insect wings, the skin friction coefficient is equal to (Schlichting 1979):

$$C_{D,sf} = 2.66\left(\frac{1}{Re^{0.5}}\right) \quad (5)$$

Because, at low and intermediate Reynolds numbers, skin friction may attenuate lift while adding a significant amount of drag, the total force vector tilts backwards on the wing surface (in addition to the induced drag effect) in the direction of the fluid motion. As a consequence of viscous drag, the orientation of the mean force vector θ_F with respect to the centre line of the wing profile, and thus the amount of lift that a wing produces, depends on the ratio between lift and drag coefficient given by (Dickinson 1996):

$$\theta_F = \alpha_g + \tan^{-1}\left(\frac{C_L}{C_D}\right) \quad (6)$$

In the 'quasi-steady' approach, the force coefficients C_L and C_D are time-invariant. They are derived typically from experiments in which model wings are tested in wind tunnels or flow tanks at different angles of attack and over the range of flow velocities that the wing encounters during flapping wing motion. Assuming that in a flying insect the wings encounter at each stroke position 'quasi-steady' flow conditions similar to those in a wind tunnel or flow tank, lift and drag can be estimated roughly throughout the stroke cycle from kinematic studies that provide wing velocity and the geometric angle of attack. To take into account that wing velocity and wing chord changes from wing base to tip, the elementary blade approach integrate the force produced by each thin wing slice spanwise (Ellington 1984e). Integrating lift over the entire stroke cycle eventually gives total lift production of the flapping wings.

Most of the discrepancy between calculated and measured flight forces in insect flight is due to the time-averaged estimates of lift and drag coefficients in wind tunnels assuming steady-flow conditions. Lift coefficients derived under those conditions typically yield values around 1.0, such as 0.93–1.15 for dragonflies' wings (Newman et al. 1977; Okamoto et al. 1996; Wakeling and Ellington 1997b), 0.86 for the crane fly *Tipula oleracea* (Nachtigall 1977), 0.7–0.87 for the wings of the fruit fly *Drosophila* (Vogel 1967b; Zanker and

Götz 1990) and 0.69 for the wings of the bumble bee *Bombus terrestris* (Dudley and Ellington 1990b). In contrast, during flapping motion, the wing coefficients undergo a complex time history in which time-variant unsteady phenomena may enhance the coefficients. Moreover, these non-steady effects are not limited to the translational parts of the stroke (up- and down-stroke) but may also occur near the end of each half stroke (ventral and dorsal stroke reversal) when the wings are quickly rotated around their spanwise axis (Chadwick 1940; Dickinson et al. 1993; Ennos 1988b; Wakeling and Ellington 1997a; Willmott and Ellington 1997a, 1997b; Zanker 1990a). Thus in many instances, lift coefficients estimated from direct force measurements in flying insects are significantly larger than those predicted by the quasi-steady approach, ranging from approximately 1.2 to 4 in various insects such as the hawkmoth *Manduca sexta*, bumble bee *Bombus terrestris*, parasitic wasp *Encarsia formosa*, dragonfly *Aeschna juncea*, and the fruit fly *Drosophila melanogaster* (Ellington 1975, 1984e; Lehmann and Dickinson 1998; Norberg 1975a; Weis-Fogh 1972, 1973). Although time-invariant lift and drag coefficients offer only a little insight into aerodynamic mechanisms, they are useful terms for comparison allowing us to quickly estimate the contribution of non-steady aerodynamic mechanisms to lift production in flying animals.

Vorticity and circulation

A more powerful concept to help in understanding the production of aerodynamic forces and wake structure is the concept of *circulation*. Circulation around a wing is a mathematical model that derives lift and drag estimates from the differentials in fluid velocity generated by flow asymmetries in translating or rotating wings and is closely related to *vorticity* (Fig. 2a). Both quantities describe rotational motion in fluids: vorticity describes the rotation of a fluid element at a point (point vortex) while circulation is the total amount of vorticity passing through any plane region within a flow field (von Mises 1959). In a fluid motion, different fluid particles may have different vorticities, and the vorticity of a fluid element may change when the fluid element is moving along the wing. Whenever fluid velocities change over a small spatial distance, vorticity becomes large. Without local changes in fluid velocity, a translating wing would not produce any vorticity, and thus circulation and force production would be zero.

Mathematically, vorticity is defined as the curl of a velocity vector in the fluid about all three dimensional axes and is equal to twice the angular speed of a local fluid particle. Therefore vorticity has the dimension of the inverse of time. The reason that moving wings may produce vorticity is due to the *viscosity* of the fluid. Since vorticity relies on changes in fluid velocities, most of the vorticity of a translating wing may be generated within the boundary layer around the wing. The boundary layer

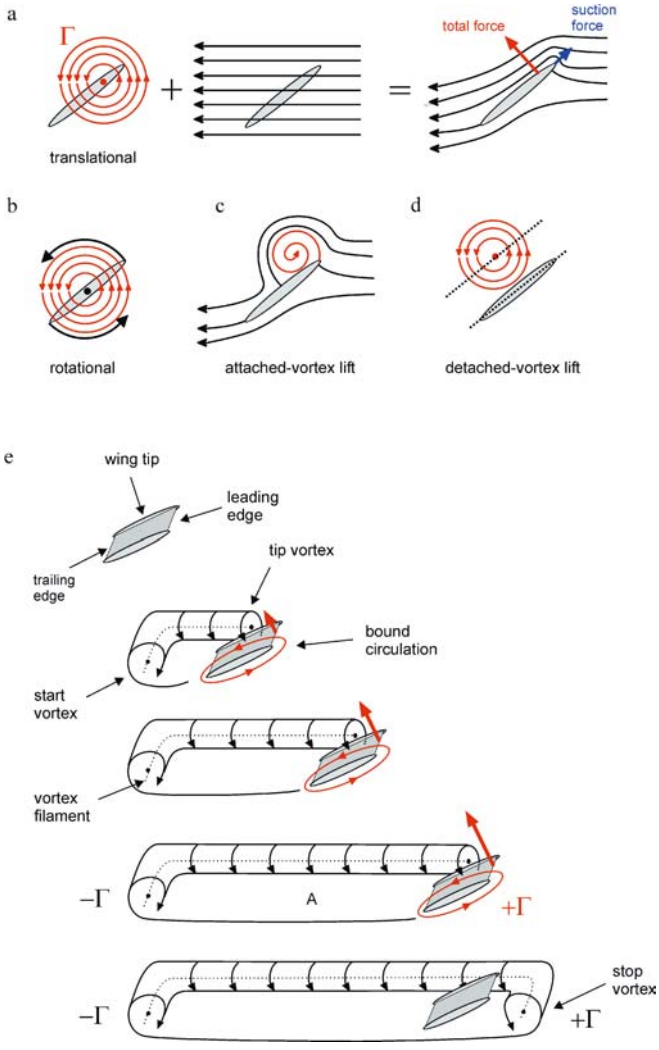

Fig. 2a–e Various types of aerodynamic circulation in aerofoils. **a** Kutta circulation (Γ, *left*) due to wing translation (*middle*) at low angle of attack. Total force production is proportional to the product of circulation and translational velocity. Stream lines (*black*) around the wing indicate a frontal and rear stagnation point near the wing's leading and trailing edge, respectively. **b** Wing rotation induces rotational circulation that may enhance force production when the wing is translating. **c** A leading-edge vortex may form at high angle of attack during wing translation which enhances lift production. The flow separates from the leading wing edge and reattaches on the dorsal wing surface. **d** A detached vortex captured from the surrounding fluid may enhance lift during wing translation (see Polhamus 1971). **e** Vortex system and development of bound circulation in an aerofoil starting from rest. The delay in maximum lift production (*red arrow*) is due to the separation between start vortex and bound circulation. When the wing stops its motion-bound circulation is shed as a stop vortex into the wake. *A*= area of vortex loop

is a thin layer of fluid that is attached to the wing's surface and is thus an interface between a solid body and its surrounding fluid. In this transition region, fluid velocities increase from zero near the wing surface (no slip condition) to the free stream velocity further away from the wing. The velocity gradient within the boundary layer induces vorticity that we consider as an infinitely

small point vortex of a local fluid element. The motion of the point vortex is driven by shear stress between the different fluid layers within the boundary layer. Since vorticity is defined as a point vortex, it induces circular fluid motion around this point with a radial velocity that is equal to the product between angular velocity of the spin ω times the distance r from the vortex core (rotational flow). The strength κ of this point vortex is then defined as the product between the radius of the concentric circles around the vortex core times radial velocity, yielding (von Mises 1959):

$$\kappa = \omega r^2 \tag{7}$$

Seen in space, the rotating core of the point vortex forms a thin cylinder of fluid termed a *vortex filament* (Fig. 2e). Circulatory fluid motion may be conceived as attached to this straight vortex filament of the vorticity κ and can be found by integrating the tangential components of the velocity vectors around the point vortex along a line that encloses the entire vortex. Outside the vortex filament, fluid velocity decreases with increasing distance from the filament due to fluid viscosity (irrotational flow) similar to the velocity gradient of the boundary layer. Thus circulation Γ is proportional to the product between the circumference of the point vortex and its induced velocity and can be expressed using Eq. 7 as

$$\Gamma = 2\pi\kappa \tag{8}$$

with the dimension of length squared per unit time. In summary, circulation is a selective measure of the strength of the flow *around* a wing but tells nothing about the components of motion perpendicular to the enclosed area or flow that averages to zero around the wing. Every non-circulatory flow, such as fluid velocity components that are parallel to the direction of wing motion, do not contribute to circulation. This can be shown by subtracting those flow components parallel to the direction of wing motion from the velocity field that a translating wing produces while generating aerodynamic forces (Fig. 2a).

The phenomenon of lift: the Kutta condition

In the previous paragraph I showed that circulation around a translating wing is due to vorticity generation in the boundary layer. Although this is a major step forward in understanding the aerodynamic basis of force production in insect wings, we still need to know the relationship between the production of upward lift and the magnitude of circulation. Since circulation depends on flow velocity, larger circulation coincides with smaller pressure forces above the wing surface pulling the wing in an upward direction. If we consider circulation in Fig. 2a in a counter-clockwise direction around the foil, the relationship between upward lift production per unit wing span L_c and circulation is given by the Kutta-Zhoukowskii theorem, that is

$$L_c = \rho u \Gamma \tag{9}$$

Combining the relationship above with the steady-state formulation of lift production in Eq. 1, we can express the dimensionless lift coefficient for force generation in terms of circulation normalised to wing speed and wing geometry that yields

$$C_L = 2\Gamma u^{-1} c^{-1} \tag{10}$$

In a non-viscous ideal fluid that exhibits *potential* flow, circulation may take on arbitrary values because there is no fluid viscosity and thus no vorticity generated in the boundary layer that fixes circulation to a certain value. In viscous (real) fluids, however, a single solution exists for circulation if the Kutta condition applies.

Let us consider the actual physics of the flow in order to completely comprehend lift as a fluid dynamic phenomenon attributed to viscosity of a fluid. We start with a resting aerofoil in a viscous fluid (Fig. 2e). At the instant motion starts, the flow is potential (inviscous) and we measure extremely large fluid velocities near the trailing edge of the wing. There are two points of stagnation where fluid velocities are zero, dividing the stream lines into parts above and below these points (Fig. 2a). After this initial phase, the velocities between the rear stagnation point and the trailing wing edge decrease slowly to zero because of fluid viscosity and static pressure increasing as predicted by Bernoulli's equation for inviscous incompressible irrotational flow. The shear stress within the boundary layer acts against this high pressure zone, moving the rear stagnation point towards the trailing edge. Chaplygin (1909, cited in Chaplygin 1956) hypothesised that the flow occurring under these conditions is that with a finite velocity at the trailing edge. In other words: only circulation of a certain strength is able to hold the rear stagnation point at the trailing edge of the aerofoil which is termed the Kutta-Zhukowskii condition. Thus the circulation that a moving wing generates at a certain speed and angle-of-attack is the Kutta circulation. However, the Kutta condition applies only for aerofoils with a sharp trailing wing edge, such as most insect wings and conventional aerofoils. In cases in which the trailing wing is rounded, the flow becomes more complicated and circulation is no longer fixed by the Kutta condition.

At this point we have to introduce Kelvin's theorem that in a system with no dissipative forces (no viscosity), circulation around a closed curve is conserved for all times or in other words: the net circulation of an irrotational flow in a closed system (flow region) cannot change, whereas in contrast the net circulation in a fixed region may change through time. If there is no circulation present in the fluid when the aerofoil rests, total circulation in a closed system must stay zero even when the wing is moving. Superficially this law sounds paradoxical because a moving wing may generate circulatory lift, as we have learned above. The answer to this puzzle is that within a fluid region there may exists *two* vortices with circulation exactly similar in size and strength but with opposite spin (sign). The generation of circulation bound

to the wing thus does not violate Kelvin's law of angular momentum conservation, assuming a pair of vortices. A wing starting from rest leaves behind a mirror image of the developing circulation bound to the wing which is called a *starting vortex* (Fig. 2e). This vortex grows in strength as long as the rear stagnation point moves towards the trailing edge while the wing builds up its full lift and is lost (shed) eventually into the wake. Thus, the size of the vortex as seen on a runway behind a starting aeroplane reflects the amount of circulation that the wings produce during take-off. The Kutta condition also predicts that after a complete stop the wing must shed all its bound circulation as a free *stopping vortex* that is equal in strength to the starting vortex. Both starting and stopping vortices can be visualised in the wake behind flying animals or flapping robotic wings and tell aerodynamicists how much bound circulation an aerofoil may have produced after its initial start (Brodsky 1994; Ellington 1984d; Grodnitsky and Morozov 1993; Rayner 1979; Rayner et al. 1986). Eventually starting and stopping vortices slowly diminish in strength because of fluid viscosity and become absorbed by the flow heating up the fluid around the moving wing.

Up until now we have considered the starting and stopping vortex, and bound circulation in only two dimensions. Under these conditions the circulatory system can be considered according to Kelvin's law as a system of two point vortices: the vortex (circulation) bound to the wing that eventually becomes a stopping vortex, and the starting vortex (Fig. 2e). In a three-dimensional space, however, vortices or vortex filaments can not exist freely (Milne-Thomson 1966). Either they have to be attached to a fluid–surface interface such as the wing or the body of the animal or they must be connected to its other end to form a continuous vortex ring. Thus the wings of a gliding butterfly may create a single continuous vortex loop formed by the vorticity filament of the bound circulation and the filament of the starting vortex (Brodsky 1991, 1994; Ellington 1984d). In flapping flight, the vortex loop is formed by the starting and stopping vortex shed at the beginning and the end of each half stroke that are connected via tip vortices. Tip vortices are created in finite wings by flow that follows the pressure gradient between the lower (high pressure) and the upper (low pressure) wing surface. Grodnitsky and Morozov (1993) have investigated the air flow around the wings of six insect species using *Lycopodium* spores and found that those animals create a single vortex ring during a complete stroke (vortex generation during the down-stroke) and refuted the hypothesis suggested by other authors that the wake consists of vortex rings connected by their upper and lower parts in a chain (Brodsky 1991, 1994; Ivanov 1990). A single vortex ring per stroke cycle shed parallel to the wing's stroke plane also agrees well with the results reported by Ellington (1980) on insects and results of flow visualisation experiments on slowly flying birds (Kokshaysky 1979; Spedding 1986; Spedding et al. 1984).

The significance of advance ratio

Over the past decades it has become increasingly clear that the lift coefficients derived under steady flow conditions in the wind-tunnel are too small to explain why many insects may produce more lift than predicted by conventional fixed-wing aircraft aerodynamics (see paragraph on quasi-steady approach). The validity of this statement, however, critically depends on the errors associated with the estimations of the fluid velocity over the flapping wing. This vector is given by the vector sum of two separate factors: the velocity u_w with which the insect flaps its wings up and down and the animal's forward speed u_f that adds to flapping velocity. The ratio between both measures is termed advance ratio J and is simply given by (Walker 1925):

$$J = u_f u_w^{-1} \tag{11}$$

The advance ratio provides an estimate of how much circulation an animal may gain from its own forward speed compared with the circulation produced by the flapping wing motion. An advance ratio of zero indicates hovering flight because all circulation is generated during the four phases of wing motion: the two translational phases (up- and down-stroke) and two rotational phases (supination and pronation) at the end of each half stroke when the wings are quickly turned around their longitudinal (spanwise) axis (Chadwick 1940; Dudley and Ellington 1990a; Ellington 1984b; Ennos 1989; Götz 1987; Nachtigall 1979; Tu and Dickinson 1996; Vogel 1967a; Wakeling and Ellington 1997a; Willmott and Ellington 1997b; Zanker 1990a, 1990b). At high advance ratios, the flow conditions are dominated by the forward flight speed rather than by the wing's own flapping velocity and in many instances conventional 'quasi-steady' aerodynamics becomes applicable to insect flight (Jensen 1956; Weis-Fogh 1972, 1973). Despite the fact that even moderate forward speeds might significantly contribute to lift, because lift depends on velocity *squared*, a maximum lift coefficient below 1.0 as determined in the wind tunnel experiments for most insect wings is not necessarily high enough to support the animal's body weight.

In a tethered flying fruit fly *Drosophila*, for example, maximum flight forces are generated at a maximum wing velocity of 1.76 m s^{-1} (Lehmann and Dickinson 1998) At this wing velocity, stroke amplitude has reached its morphological limit near 180° while stroke frequency is slightly below its maximum value due to power constraints of the asynchronous flight muscles (Lehmann and Dickinson 1997). Under these flight conditions the quasi-steady model would require a lift coefficient of 1.9 to explain the measured flight forces, but the steady-state lift coefficient measured in the wind tunnel value is 0.8 (Lehmann and Dickinson 1998; Zanker and Götz 1990). Assuming that maximum force production in the tethered animal would allow a freely flying fruit fly to cruise with a forward flight speed of 0.5 m s^{-1}, which is at the high

end of the speeds observed, the animal gains potentially 1.7 times more lift due to an increase in wing velocity (David 1978). However, even an 1.7 times increase in lift production due to the insect's forward motion would not be sufficient to sustain active flight in this fly species, assuming the steady-state lift coefficient of 0.8. Consequently, even at fast forward flight it is likely that some insects employ unsteady aerodynamic mechanisms for active flight.

A low advance ratio also potentially favours the three-dimensionality of flow structure on the moving wings. To dissect the fluid dynamic conditions at high and low advance ratios, I like to start with gliding flight (infinite advance ratio) and make some inherent assumptions on wing geometry and motion. Wings that purely glide (translate) through a fluid face the same fluid velocity at both the wing tip and the wing base. Assuming no fluid dynamic effects from the wing tip ('infinite wing') there is only little interaction between adjacent wing segments, and the flow tends to be two-dimensional. At low advance ratios or hovering flight, in contrast, wing velocity significantly increases from base to tip, which may result in an increase of the pressure differentials between the upper and lower side of the wing. Although the actual pressure distribution on the wing depends on several factors including the spanwise distribution of wing chord, the increasing pressure differentials in a generic insect wing should cause that fluid velocity differentials to increase likewise. The pressure difference between two chordwise pressure zones produces a spanwise flow of the fluid, termed *axial flow*, which is thought to be directed towards the wing tip on the upper wing surface and towards the wing base on the lower surface (Fung 1993). On the upper wing surface, centrifugal forces might even enhance spanwise flow while axial flow on the lower side would be attenuated. Axial flow on the upper wing surface might be an important factor for stabilising vorticity produced at the leading edge of insect wings at intermediate Reynolds numbers, and this will be discussed in the following paragraphs.

Leading-edge vorticity

General introduction

The general view on insect flight describes lift production as the result of aerodynamic phenomena occurring during the translational parts of wing motion (Buckholz 1981; Hoff 1919; Hollick 1940; Holst and Küchemann 1941; Weis-Fogh 1956). Lui et al. (1998), for example, writes that in the hovering hawkmoth *Manduca sexta*, "estimation of the forces during a complete flapping cycle shows that the lift is produced mainly during the down-stroke and the latter half of the up-stroke, with little force generated during pronation and supination" when the wings rotate at the end of their dorsal and ventral excursion, that supports the general assumption. But how can a wing that is moved by the insect significantly produce more force than a wing in a wind tunnel that faces the same flow velocities? The search for the answer to this question has driven the discovery of leading-edge vorticity in flying insects.

The discovery of the leading-edge vortex (LEV) in a flying insect closely links biology to engineering because the potential of trapped or wing attached vortices for lift enhancement has long been recognised in aerodynamics (Bradley et al. 1974; Campbell 1976; Dickinson and Götz 1993; Dixon et al. 1973; Gleason and Roskam 1972; Krall and Haight 1972; Kruppa 1977; Maxworthy 1979; Rossow 1978; Sunada et al. 1993). A comprehensive review on the physics of vortex lift is given by Wu et al. (1991). Superficially a vortex may enhance flight forces by adding its own vorticity to the circulation bound to the wing during translation. This coincides with structural changes in the flow around the wing. The LEV is a prominent example of an attached vortex because its initiation and stability has been investigated in great detail in both insect wings and aerofoils of aircraft (Ellington et al. 1996; Houghton and Carpenter 2003; Katz and Plotkin 2002; Usherwood and Ellington 2002a; van den Berg and Ellington 1997).

To understand the changes in flow due to leading-edge vorticity, we consider the laminar flow around the leading edge of a wing travelling at a low angle of attack through the air. Under these conditions the fluid follows the wing contour smoothly around the leading edge whereby the flow 'sticks' to the wing surface (attached flow). The location of the frontal stagnation point requires that the fluid is accelerated around the leading edge region that is associated, according to Bernoulli's equation, with a low pressure domain termed 'leading-edge suction' (Fig. 2a, Fung 1993; Polhamus 1971). Although, in aeronautics, the leading-edge suction analogy is used primarily to develop analytical models predicting low-speed lift of sharp-edge delta wings, the concept has also been used to understand fluid-dynamic phenomena in insect flight (Dickinson and Götz 1993; Usherwood and Ellington 2002a). The analogy assumes that the normal force required to maintain the reattached flow on the upper surface of the wing is the same as that required to accelerate to flow around the leading edge. The part of the suction force that is parallel to the direction of wing motion thus counterbalances pressure drag that acts into the direction of flow. The vertical component of the leading-edge suction adds to lift and helps to keep the insect in the air. However, in flight this situation can only be obtained by wings operating at low angles of attack with blunt leading edges that accelerate the flow gradually (Katz and Plotkin 2002).

In contrast, at a high angle of attack, when the flow around the leading edge no longer follows the wing contour smoothly, a leading-edge vortex may develop. Under these conditions the local viscous forces within the fluid are smaller than the pressure forces associated with high fluid velocity and the flow separates from the upper surface of the wing. Thin aerofoils, such as most insect wings, even favour fluid separation because the flow

acceleration around a sharp leading edge requires a higher pressure gradient than in rounded (blunt) edges. The low-pressure region behind the leading edge in turn induces flow to curl back and to reattach subsequently on the upper side of the wing posterior of the leading edge. This reattachment is indicated by a stagnation point (zero flow velocity) on the upper wing surface which is absent in a detached 'trapped' vortex (Fig. 2c, d; Rossow 1978). As a result of the change in pressure distribution due to leading-edge vortex formation, the leading-edge suction force vanishes and the wing experiences a substantial increase in both lift and drag (Polhamus 1971).

In conventionally shaped (blunt) wings of aircraft flying at high Reynolds number the flow attached to the wing starts to separate when the angle of attack exceeds a critical value of 12–15° (Katz and Plotkin 2002). When the flow separates from the entire upper wing surface, the wing stalls completely and circulation is shed into the wake, causing a complete loss of lift. Thus a leading-edge vortex structure that has been formed at angles above 12–15° is thought to be a temporary non-steady aerodynamic phenomenon and its benefit termed *attached-vortex force* may be limited to a short time window (Kuethe and Chow 1986). Dynamic stall occurs in aerofoils when the wing pitch is oscillating around the critical angle (Ham and Garelick 1968; Silcox and Szware 1974; Stepniewski and Keys 1984). This causes a periodic initiation and shedding of strong vortex-like disturbances from the leading edge region, preventing the wing from stalling completely (McCroskey et al. 1976). Other experiments have shown that at intermediate Reynolds numbers of around 200, lift production following an impulsive start of a insect model wing at high angle of attack is approximately twice the steady-state value (Dickinson and Götz 1993). However, this enhanced lift relies on unstable leading-edge vorticity and thus quickly drops when the wing stalls, while moving further through the fluid.

The benefit of generating a leading-edge vortex resides in its capacity to effectively increase the camber (curvature) of a wing that adds vorticity (and thus lift) to circulation produced by the Kutta-condition during wing translation. In aircraft design, a widely known application of leading-edge vorticity are thin delta-shaped wings such as the wings of the Concorde and other military jets (Katz and Plotkin 2002). Delta-wings stabilise leading-edge vortices due to their pressure gradient spanwise, increasing lift well above the critical angle of attack. Under those flow conditions, lift coefficients may range from 4 to 6 (Wu et al. 1991). Prediction from analytical models on circulation generated by 'trapped' vortices on the upper wing surface even suggests maximum lift coefficients ranging from 5 to 9.5; that is, up to 10 times higher than during conventional flow conditions (Rossow 1978). For example, at maximum angle of attack of 14° at which flow remains attached, and assuming the largest theoretical prediction of 2π for the lift coefficient slope in a translating elliptic thin aerofoil following the Kutta-condition, this would result in a lift coefficient of approximately 1.5, which demonstrates the enormous potential of vortices associated with moving wings for lift enhancement (Kuethe and Chow 1986).

Physical models

A three-dimensional leading-edge vortex in an insect has been described in great detail in a tethered flying hawkmoth *Manduca sexta* and dragonflies (Ellington et al. 1996; van den Berg and Ellington 1997; Willmott et al. 1997; Reavis and Luttges 1988). By using smoke streams to visualise the wake around the moving wings, Ellington and colleagues were able to demonstrate the presence of a vortex close to the leading edge of the moth wing. At low head wind (0.4 m s^{-1}) which compares to slow forward speed of the moth, the vortex is small and the wake is quite unstable. With increasing speed (up to 5.7 m s^{-1}) the leading-edge vortex grows in size and eventually extends over the entire wing surface (Fig. 3a). Unfortunately, the visualisation results for flow in tethered flying insects are not clear enough to derive good flow reconstructions near the flapping wings. Moreover, in tethered flight it is difficult to measure forces and moments produced by the animal wings in all six degrees of freedom and with temporal resolution sufficiently high to link wake structure and aerodynamic force production. Thus, over the last few decades several biologists and aerodynamicists have developed mechanical models of insect wings in order to study the wake around an insect in greater detail.

Bennett (1970) presented a simple three-dimensional mechanical model wing based on the beetle *Melolontha vulgaris* that allowed wing incidence to change while flapping the wing back and forth in the stroke plane. Maxworthy's (1979) three-dimensional wing allowed us to study the flow around model wings at the beginning of the down-stroke but did not allow us to actively change the angle of attack while flapping. Spedding and Maxworthy (1986) used a two-dimensional model that could only rotate the wings but allowed us to measure aerodynamic forces on the wing via a load cell (force transducer). Physical models for investigating dragonfly aerodynamics were employed by Saharon and Luttges (1987), Kliss et al. (1989) and Savage et al. (1979). A major progress in robotic wing design was made by Ellington et al. (1996), who constructed two robotic wings that allowed continuous wing flapping. The wing motion was controlled by a computer that mimics wing motion based on the kinematics of the hovering hawkmoth. The model is approximately 10 times larger than *Manduca* and flaps its wings in air at a frequency of 0.3 Hz. Although the 'flapper' is a useful concept for studying the effect of wing kinematics on the structure of the wake, its benefit was limited because it was not originally equipped with a force sensor that allowed the measurement of aerodynamic force production during the stroke. More recently, biologists have presented a two-winged robotic apparatus ('robofly') that is driven by an assembly of computer-controlled stepper motors attached to a wing gear box via timing belts (Dickinson et al. 1999; Lehmann 2000). Each

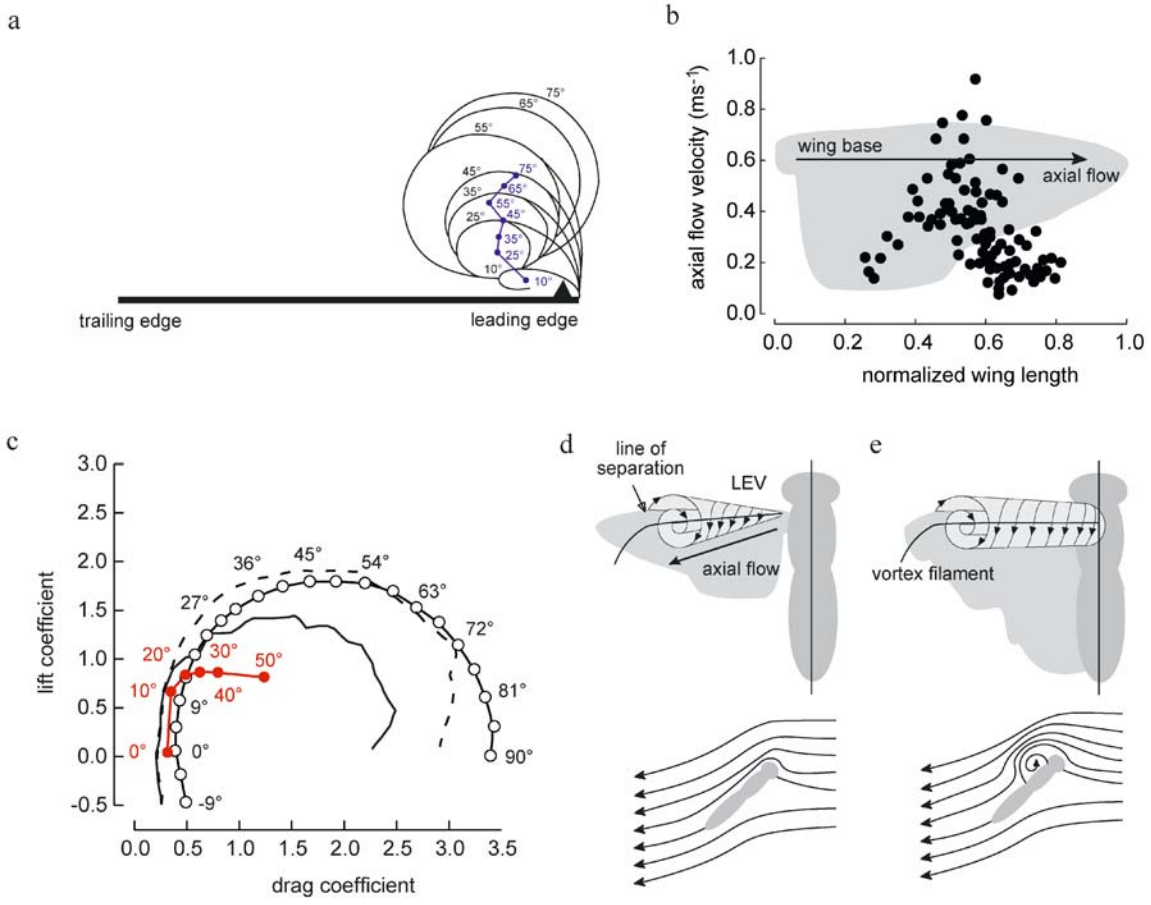

Fig. 3 **a** Size of leading-edge vortices on the upper surface of a moving dynamically-scaled robotic model wing at 50% wing length of the hawkmoth *Manduca sexta*. The vortex size increases with increasing angle of attack from 10° to 75° while the vortex core (*blue*) moves away from the upper wing surface (modified from van den Berg and Ellington 1997). **b** Axial flow velocities within a leading-edge vortex on a hawkmoth model wing during 'hovering' flight (modified from Ellington et al. 1996). **c** Steady-state lift and drag coefficients (*open circles*) as a function of the geometric angle of attack during wing translation in a three-dimensional fruit fly model wing. Coefficients were calculated using a quasi-steady elementary blade approach. *Superimposed lines* show the steady-state (*solid*) and transient coefficients (*broken*) of a two-dimensional robotic wing moving at similar Reynolds number of 134. Steady-state coefficients of fruit fly wings estimated in a wind tunnel are *plotted in red* (Vogel 1967b). **d** Schematic of the conical and helical structure of a leading-edge vortex in the hawkmoth due to axial flow. During hovering flight there is no vortex on the animal body (*lower image*). **e** In a butterfly during take-off in a wind tunnel, the helical flow of the leading-edge vortex is absent and the vortex expands across the midline of the animal's body (*lower image*). Under those conditions axial flow appears to be small or absent (modified from Srygley and Thomas 2002)

wing was capable of rotational motion about three axes and was immersed in a tank of mineral oil. The viscosity of the oil, the wing length and the speed of the wing were chosen to match Reynolds number typical for the flight of the fruit fly *Drosophila melanogaster* (*Re*= 134). The base of the wing was equipped with a two-dimensional force transducer that allowed the measurement of shear forces, not bending moments, normal and perpendicular to the wing. From a geometric viewpoint, lift and drag could be derived from these forces throughout the stroke cycle and eventually linked to the wake structure generated by the moving wings. Both the 'flapper' and the 'robofly' have provided new insights into the generation of a leading-edge vortex in insect flight and how this vortex is stabilised throughout the stroke.

Vortex strength

Seen in space, the leading-edge vortex attached to a flying hawkmoth wing or the wing of the 'flapper' is a conical spiral (helical vortex), enlarging as it is swept by the wing and stabilised by *axial flow* (Fig. 3d). The strong axial flow is due to the pressure gradient from wing base to tip and continuously removes energy from the vortex core spanwise, keeping the vortex relatively small and the flow stable (Fig. 3b). According to Helmholz's second theorem, the leading-edge vortex filament must extend across the midline of the insect body towards the wing on the other side of the animal's body or attach close to the base of the wing, where wing velocity and vorticity is small (Fig. 3d, e). From base to tip the leading-edge vortex increases in size (diameter) up to a distance of 60–70% of

the wing length, at which the vortex breaks down and lifts away (separates) from the wing surface joining the wing-tip vortex (van den Berg and Ellington 1997). At breakdown the vortex has reached its critical size, pressure force overcomes viscous forces of the fluid, and axial flow can not longer guarantee its integrity. The circulation of a leading-edge vortex Γ_{le}, as seen as a cross-section of the conical spiral, is proportional to the vorticity generated by its rotational speed (vortex swirl) u_θ and the mean vortex diameter d_{le} and is equal to

$$\Gamma_{le} = \pi d_{le} u_\theta \tag{12}$$

By spanwise tracking of smoke blobs released at the wing base in the hawkmoth 'flapper', van den Berg and colleagues estimated the helix angle within the conical spiral to be near 45°, suggesting that the magnitude of the vortex swirl is equal to axial flow velocity (Fig. 3b; Ellington et al. 1996; van den Berg and Ellington 1997). Leading-edge vortices are large structures and in the hawkmoth they reach a maximum diameter of up 70% of the wing chord. Thus their contribution to total lift production is quite remarkable. To support the weight of a hovering the hawkmoth in free flight a steady-state lift coefficient of 1.8 is required (Willmott 1995). Since the maximum steady-state lift coefficient measured in a wind tunnel is only 0.6–0.7, two-thirds of the overall performance of the flapping wing is thought to be due to leading-edge vorticity. Slightly smaller values were obtained in a robotic model based on *Drosophila* kinematics (~45%, Dickinson et al. 1999; Fig. 3c). In sum, leading-edge vorticity is induced in insects when the wings translate through the air at high angle of attack (typically 20–50°). It requires that flow separates from the leading edge and reattaches on the upper wing surface. Due to both vortex strength and size, a leading-edge vortex may far outmatch conventional aerodynamic mechanisms based on fixed-wing aircraft theory. Although leading-edge vorticity can not explain all circulation generated during oscillatory wing motion its discovery has general implication on our understanding how animals fly.

Vortex stability and axial flow

There is a ongoing controversy about the mechanisms that hold (or trap) a leading-edge vortex in place on the upper wing surface of an insect. Several technical solutions have shown directly that axial flow is the predominant factor in leading-edge vortex stabilisation at high Reynolds number. In conventional aircraft, axial flow can be created by generating an artificial air jet towards the wing tip that removes vorticity from the vortex-like flow, preventing the flow from separating fully from the wing (Rossow 1978). In the hawkmoth and the hawkmoth model wing, axial flow is clearly present and akin to the flow found in delta-winged aircraft (Willmott et al. 1997). The leading-edge vortex remains stable even in a continuously 'revolving' hawkmoth wing (propeller) that avoids confounding effects from wing rotation (pronation and supination) at the end of each half stroke (Usherwood and Ellington 2002a). In the three-dimensional physical *Manduca* model the LEV is generated as soon as the wings starts to revolve and produces maximum lift coefficients well above the two-dimensional steady-state coefficient obtained in a wind tunnel (Usherwood and Ellington 2002b). According to these results, the LEV in the hawkmoth might be described as a *steady* unsteady aerodynamic phenomenon.

Interestingly, in helicopter and wind turbine blades, axial flow is small or absent although those systems are very similar to the revolving hawkmoth model and are often compared with the up- and down-stroke in flying insects (De Vries 1983; McCroskey et al. 1976). There are three possible explanations for this discrepancy. First, helicopter and wind turbine blades rotate at high Reynolds numbers well above the hawkmoth model that flaps or rotates its wings at Reynolds number of about 7,000. Flow at high Reynolds numbers tends to be more turbulent because viscous forces of the fluid are small compared to the pressure forces. This easily causes turbulences in the fluid, and both LEV and axial flow might be minimal under these conditions. Second, in comparison with long and slender helicopter and wind turbine blades, insect wings have a small aspect ratio that is defined as the ratio between wing length and the mean chord width of the wing (Ellington 1984a; Vogel 1994). Low aspect ratio wings could facilitate the induction of LEV and axial flow that might explain the geometry of most of the wings we find in different insect species. Third, helicopter and wind turbine blades are generally given a twist from base to the tip so that the angle of attack is not constant all over the span (Stepniewski and Keys 1984; von Mises 1959). This decrease in the angle of attack towards the wing tips is called *washout* and helps to concentrate the lift in much the same way as the spanwise decrease of chord length: a comparatively larger part of the total lift is contributed by the central portion of the wing and therefore bending moments at the wing roots will be smaller for the same total lift (von Mises 1959). These modifications of the wing might alter the Bernoulli suction towards the wing tip that could potentially result in a decrease in spanwise axial flow. An exact explanation, however, of how axial flow is generated in different aerofoils moving at different trajectories and Reynolds number regimes remains uncertain.

The requirement of axial flow for leading-edge vortex stability akin to that produced by delta-wing aircraft was questioned recently by experiments using model wings based on the fruit fly *Drosophila* (Birch and Dickinson 2001). In contrast to the hawkmoth model, the spanwise flow within the LEV core of the fruit fly model ('robofly') is quite small and amounts to only 2–5% of the average tip velocity. Quite different from the outward flow at the leading edge, at the rear two-thirds of the wing there is strong spanwise flow that approaches peak velocities of 40% of the wing tip velocity. However, despite of this strong outflow of fluid there is no indication of spiral flow analogous to the helical LEV

as found in the hawkmoth. Nevertheless, in the fruit fly the relatively small velocity of axial flow within the vortex core might be sufficient to stabilise the LEV, quite similar to the flow as seen in the hawkmoth. In order to test this idea, Birch and Dickinson employed chordwise fences that limit spanwise flow in the fruit fly model. The teardrop-shaped fences were mounted on the upper wing surface either at the leading edge or the rear region of the wing to limit axial flow within the LEV or spanwise flow at the trailing wing edge, respectively. In spite of the front barriers the LEV remains stable and thus force production does not change throughout the stroke cycle. The removal of energy out the vortex core is thus not required to stabilise the LEV in this case. The anteriorly directed fences, in contrast, elicit a 25% drop in aerodynamic force production, whereas the time course of force production remains unchanged (Birch and Dickinson 2001). Although this decrease in force production seems more consistent with the findings of LEV stability in the hawkmoth, the underlying flow structures might be different and could point to different fluid dynamic mechanisms.

The negligible effect of blocking leading edge axial flow in the three-dimensional fruit fly model rises the question of why the LEV in a two-dimensional model wing becomes unstable when the wing is translating through the fluid (Dickinson and Götz 1993). Under two-dimensional conditions, the LEV typically enlarges when the wing travels through the fluid (Dickinson and Götz 1993). The resulting low-pressure domain on the upper wing surface in turn facilitates the induction of a vortex at the wing's trailing edge in order to satisfy Kelvin's theorem. While the wing is moving forward, leading- and trailing-edge vortices may have shed alternatively into the wake, leaving behind a von-Kármán-trail of vortices that are equal in strength but have an alternating rotational spin. The wing motion of the three-dimensional fruit fly model becomes rather two-dimensional when the flow around the wing tip (tip vortex) is blocked by a wall that exactly matches the sweep of the wing (Birch and Dickinson 2001). The presence of this cylindrical wall (edge baffle) reduces axial flow and thus limits the energy removal from the vortex core. As a consequence the mean strength of the LEV increases by 14%, resulting in a 8% increase of aerodynamic force production averaged over the entire stroke cycle. However, there is no sign of von-Kármán shedding, indicating that the LEV stays rigidly attached throughout the stroke cycle (Birch and Dickinson 2001).

If it is not axial flow that stabilises the LEV in the fruit fly model what then explains its stability and constant attachment during wing translation? One hypothesis is that the momentum jet directed downwards (induced flow, downwash) by the beating wings has a potent inhibitory effect on the strength of the LEV and thus on lift production (Birch and Dickinson 2001). In order to understand this possible mechanism for LEV stabilisation, I like to dissect the flow over the three-dimensional (finite wing) fruit fly wing in greater detail. A wing that translates through the fluid at a positive angle of attack accelerates fluid around the aerofoil. This acceleration results in a pressure difference between the upper and the lower wing surface and subsequently in lift. As mentioned before, at the wing tip the fluid is following the pressure gradient from the higher energy (lower) wing side to lower energy (upper) wing side creating a circular flow termed the *tip vortex*. According to Helmholtz's second theorem, the tip vortex must either extend to infinity or attach to a boundary (the wing). The production of vorticity inside the tip vortex requires kinetic energy that stems from the power generated by the drag force of the wing. Thus tip vorticity results in an additional drag force on the moving wing termed *induced drag*. Because induced drag depends on the pressure distribution spanwise it depends subsequently on the aspect ratio AR of the wing. In a low aspect ratio wing the pressure difference between the upper and lower side of a wing segment is relatively high and thus induced drag is large. High aspect ratio wings, such as wings of sail planes, produce minimal induced drag because the pressure gradient between both sides of the wing is small (von Mises 1959). At high Reynolds numbers the dimensionless induced drag coefficient $C_{D,i}$ can be derived from the wing's aspect ratio $\mathcal{R}$ and the lift coefficient by (Katz and Plotkin 2002):

$$C_{Dj} = \pi^{-1}\mathcal{R}^{-1}C_L^2 \tag{13}$$

The kinetic energy that resides in the circulation of tip vortices induces a downward flow of fluid (downwash). This induced vertical flow changes the direction of the flow vector of the oncoming air so that the aerodynamic angle of attack becomes significantly smaller than the geometric angle, as mentioned at the beginning of this review. Birch and Dickinson (2001) pointed out that, particularly in hovering flight when the wings sweep numerous times through the same fluid disc, induced flow lowers the aerodynamic angle quite substantially. In the fruit fly model the aerodynamic angle of attack at the wing tip is almost identical to the geometric angle of attack (45°) because the pressure difference between upper and lower wing sides is very low, and thus induced flow is negligible. Towards the wing's centre, in contrast, the effective angle of attack drops to roughly one-half (21°) of the geometric angle, reflecting the strong downwash of fluid generated by the inner wing segments (Birch and Dickinson 2001). Subsequently, when an insect takes off in still air, the first stroke potentially generates the largest amount of force because induced flow is minimal. Lift then decreases in the subsequent strokes due to the reduction in aerodynamic angle of attack, assuming that the animal is not adjusting its wing kinematics to compensate for that drop in lift. In total, the downwash has a potent inhibitory effect on the strength of the LEV, and both wake vorticity from previous strokes and wing-tip vorticity limit the growth of the LEV and prolong its attachment on the upper wing surface. The stability of the LEV in the fruit fly model thus might be a consequence of an effective reduction in the angle of

attack rather than reflecting a distinct aerodynamic mechanism. The short travel distance of the fruit fly wings during up- and down-stroke of only three-quarters of a wing cannot contribute to the stability of the LEV sensu stricto. Instead, the potential benefit of a short travel distance might be that it hinders the LEV in reaching a critical size and thus reduces the risk of LEV vortex shedding during the wing's translational motion. Whether the LEV remains even stable without axial flow in a revolving *Drosophila* wing has still to be demonstrated.

Although the changes in effective angle of attack due to induced flow velocity may explain why the LEV appears to be stable in the fruit fly model, it cannot explain why axial flow inside the LEV is so small. A possible reason is the relative increase in viscous forces of the fluid with decreasing Reynolds number. The Reynolds number of moving fruit fly wings amounts to 100–250 and is thus significantly smaller than in the hawkmoth, which flies at Reynolds numbers between 7,300 and 8,100 (Willmott 1995; Willmott and Ellington 1997b). High fluid viscosity may have two effects: it hinders axial flow in following the pressure gradient from base to tip and it smoothes out disturbances in the flow that increases the stability of a vortex-like structure and thus extends the time in which a vortex remains stable during wing motion. However, studies on large red admiral butterflies *Vanessa atlanta* have recently questioned the existence of axial flow even at higher Reynolds numbers similar to those found in the hawkmoth (Srygley and Thomas 2002). This observation was made in freely flying animals in a wind tunnel. Compared to tethered flying insects or 'hovering' physical models, this approach allows us to study unsteady aerodynamic mechanisms in the behaving animal that moves through the air while quickly altering the wing kinematics on a stroke-by-stroke basis.

The reconstructions of the flow above the butterfly wings using smoke trails show the leading-edge vortex spreads out from the wing surface on the body of the animal at which the vortex maintains its strength (Srygley and Thomas 2002). In contrast to the conical LEV found in the hawkmoth, the butterfly LEV exhibits a rather constant diameter from the midline of the animal's body up to the wing tip at which the vortex joins the tip vortex (Fig. 3d, e). As a consequence of this difference in vortex shape, the vortex focus of the conical LEV (hawkmoth) is attached at the wing root, whereas in the cylindrical LEV of the butterfly there is a free-slip focus above the midline of the body. Moreover, in the presence of axial flow in the butterfly LEV the smoke lines would have been deflected from the leading edge towards the wing tip. Because this type of distortion of the flow appears to be absent in *Vanessa atlanta*, Srygley and Thomas concluded that the helical structure of the LEV is small or absent. Thus in the red admiral, axial flow might not be required to stabilise the leading-edge vortex during these observed types of flight manoeuvres.

The experimental results on the red admiral are undoubtedly valid for take-off at a free stream velocity in the wind tunnel at around 1–2 m s^{-1}. At this moment the body angle of the animal with respect to the oncoming air almost approaches 90°, which might induce flow separation on the dorsal side of the body or facilitate that the LEV expands across the midline of the animal's body towards the other wing. Moreover, the relatively high advance ratio might explain the absence of axial flow because the body of the animal, the wing base and the wing tip face similar flow velocities and Bernoulli suction that drives axial flow would be minimal. Thus, it remains open whether these findings can necessarily be carried across to cruising flight of butterflies at lower advance ratios. Despite these concerns, the main outcome of such studies is to show the repertoire of different kinematic manoeuvres and flight modes in insects and the resultant alterations in the complex flow patterns that may change from stroke to stroke. Although a comprehensive theory of LEV initiation and stabilisation covering different types of leading-edge vorticity has still to be developed, the recent results already enable us to get a deeper insight into the non-steady fluid mechanical phenomena in flapping flight.

Rotational and Magnus circulation

Leading-edge vorticity might be present in many flying insects and its stability seems not to be limited to a specific Reynolds number domain as mentioned above. In the hawkmoth *Manduca sexta* and the fruit fly *Drosophila*, Kutta-circulation due to wing translation and leading edge circulation are sufficient to explain the flight force needed to keep the insect airborne (Dickinson et al. 1999; Willmott et al. 1997). However, there are two main reasons that circulation produced during wing translation may not be the only aerodynamic mechanism that enhances flight forces in flying insects.

First, experiments conducted with tethered fruit flies flown in a virtual reality flight arena indicate that an increase in flight force production involves an increase in both the wing flapping velocity *and* the lift coefficient (Lehmann and Dickinson 1997, 1998). While wing flapping velocity increases when the wings undergo larger stroke amplitudes and/or stroke frequencies, the two-fold increase in lift coefficient between minimum and maximum locomotor capacity of the flight apparatus points towards aerodynamic phenomena that might not reside in the translation wing motion. This conclusion is supported by the finding that in the robotic *Drosophila* wing that moves with constant velocity and inclination in each half stroke, lift production and thus LEV strength is approximately constant after an initial phase of wing acceleration (Dickinson et al. 1999). Thus, it is unlikely that the increase in mean lift coefficient at elevated flight force production is attributed simply to an increase in LEV strength with increasing stroke amplitudes.

Second, direct force measurements on tethered flying fruit flies have shown that maximum forces are produced during wing rotation and not during wing translation,

suggesting that the stroke reversals might add a significant amount of force to total lift (Dickinson and Götz 1996; Zanker and Götz 1990). As mentioned earlier, insects rotate their wings around the spanwise axis at the end of the up- and down-stroke. From a kinematic point of view, this manoeuvre is required solely to obtain an adequate angle of attack for the next following half stroke. The simple 'quasi-steady' approach (Eq.1) does not predict force peaks at the end of each half stroke because, in this model, lift production purely relies on translational wing velocity that is small during the stroke reversals. Quite similar to the discovery of the leading-edge vortex, the discrepancy between the measured high lift peaks during wing rotation in the tethered flying fly and the predictions from the simple conventional aerodynamic model was tackled in a dynamically scaled robotic wing (Dickinson et al. 1999).

A possible explanation for the force peaks at the end of each half stroke is that the wing's own rotation serves as a source of circulation to generate an upward force (Fig. 4). Originally, the augmented circulatory lift has been mistaken as a result of the Magnus effect. However, this mechanism, rotational circulation, is *not* akin to the Magnus effect (sensu stricto) although both aerodynamic phenomena share similar time histories in force production and are both based on the acceleration of fluid around the rotating object. The motion of the fluid cylinder around the object is driven by the fluid's viscosity and the direction of its spin is thus equal to the rotational spin of the object (Fig. 2b; Fung 1993). The Magnus force makes a soccer-ball curve from its path towards the goal and is independent of the angle of attack and rotational moments (Sun and Tang 2002). In this sense, Magnus circulation is similar to translational circulation resulting from the distortion of the flow on a pitched wing in a uniform flow. However, Magnus circulation is independent of the chordwise centre of the incident flow and thus differs from rotational circulation. A detailed overview on the different use of the term 'Magnus-like force' for describing aerodynamic forces is given by Walker (2002b). Consequently, when a translating insect wing rotates around its longitudinal axis, it may experience both rotational and Magnus circulation. Although Magnus forces may contribute to total lift balance of an animal (Fung 1993) recent analytical models and CFD results suggest that Magnus force is not needed to explain flight forces generated during wing rotation (Sun and Tang 2002). Magnus force even makes the prediction of some analytical models worse and has thus been questioned as an important factor for lift production in insects in general (Walker 2002b).

The amount of rotational circulation produced by a rotating wing depends on the rotational axis of the wing or in other words by the length ratio between the proximal and distal wing segment (Fig. 4c). In thin aerofoils such as insect wings rotational circulation Γ_r depends on wing chord and the normalised position of the rotational axis $\hat{x}_0$, which is the distance between the axes and the leading

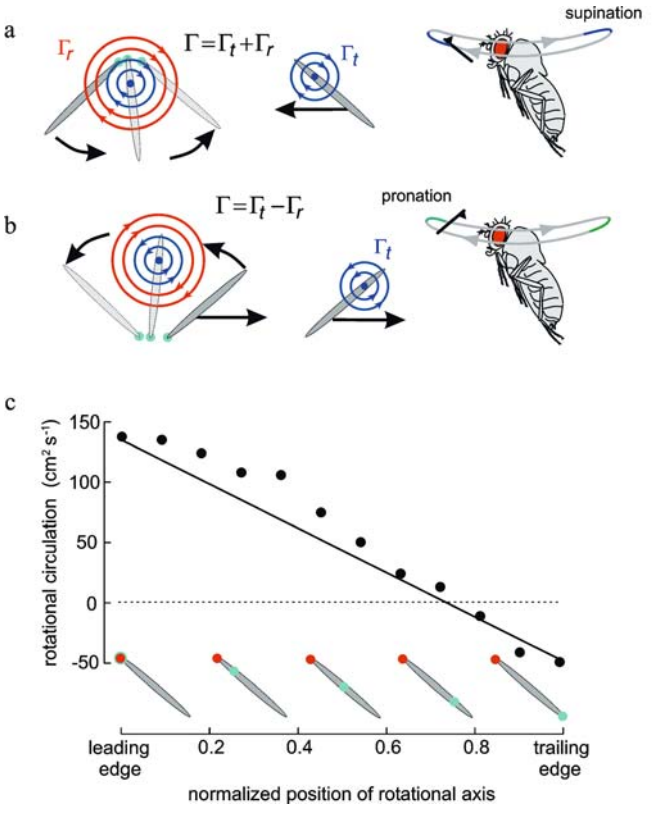

Fig. 4a–c The contribution of rotational circulation to total circulation (Γ) depends on the wing's rotational timing within the stroke cycle. **a** When the wing rotates at the end of the half stroke, rotational circulation (Γ_r) adds to circulation produced during wing translation (Γ_t). **b** When the wing rotates at the beginning of a half stroke, rotational and translational circulation have opposite spins and lift production is attenuated. *Coloured sections* of the wing tip path plotted on the right indicate the phase of wing rotation. **c** Measured values of rotational circulation are plotted as a function of the normalised position of the rotational axis in a robotic wing. The data were calculated using the total rotational force generated by an advanced kinematic pattern as shown in Fig. 5a and close to the point of peak force generation. The *solid line* indicates the theoretical prediction of circulation based on Eq. 14 in the text. Wing speed is 0.15 m s^{-1}, angular velocity is 74° s^{-1} and Reynolds number is approximately 136. *Red dots* indicate leading wing edge and *green dots* the location of the rotational axis

wing edge divided by total wing chord (DeLaurier 1993; Fung 1993). The relationship is thus

$$\Gamma_r = \pi\omega c^2(0.75 - \hat{x}_0) \qquad (14)$$

in which ω is the angular speed of the wing. A wing that rotates around the leading edge axis $(\hat{x}_0) = 0$ induces maximum circulation. In the fruit fly, the wing's rotational axis is approximately one-quarter behind the leading edge, which would result in a one-third reduction in rotational circulation. As the rotational axis moves away from wing's leading edge, rotational circulation decreases and is zero at three-quarters distance (Fig. 4c).

Detailed work on rotational axis has shown that the value 0.75 is only valid for attached flow and changes with rotational velocity when the flow is separated, which is the case in insect wings. Thus the position of the

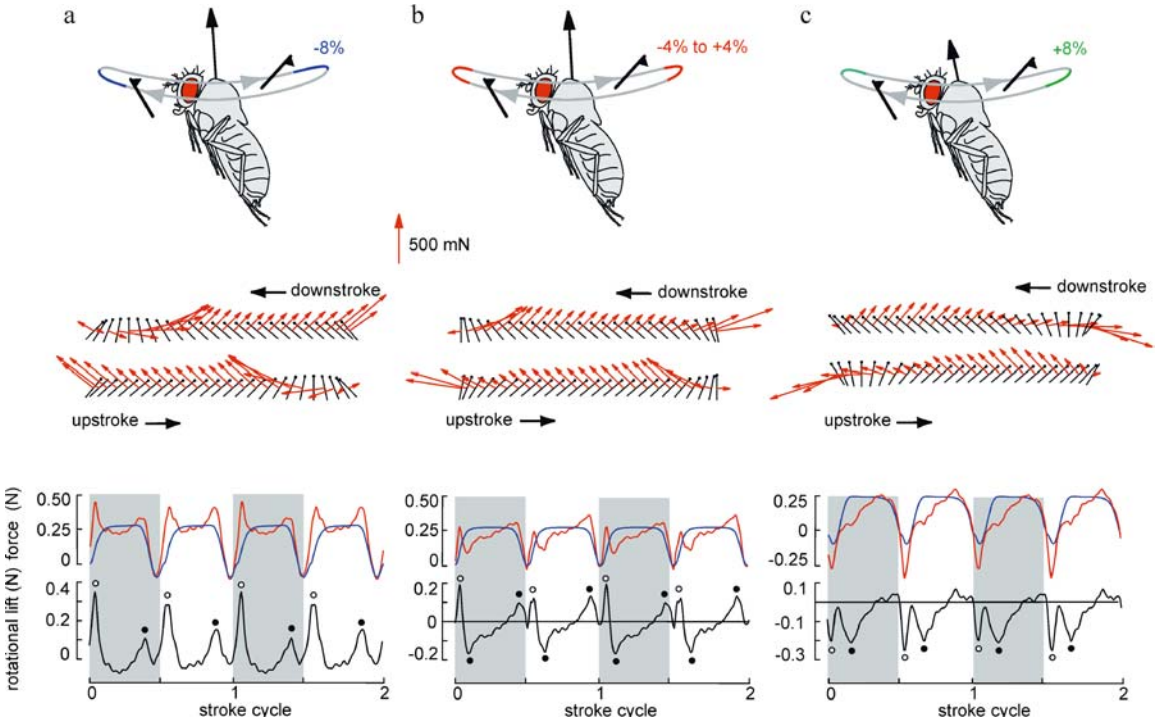

Fig. 5a–c Instantaneous forces of a model wing plotted for three types of rotational timing at stroke reversals (*upper row*) superimposed on a diagram showing wing motion (*middle row*, *black line*= chordwise wing element, *black dot*= leading edge). Effects of rotational timing on lift (*lower row*) generated for the stroke pattern as shown above. Rotational force (*black*) was derived from the difference between total force production (*red*) and forces produced during wing translation (*blue*). *Grey area* indicates the time of the wing's down-stroke. Force peaks due to rotational circulation are marked by a *closed circle*, force peaks due to wake capture or added mass are marked by a *hollow circle*. **a** Advanced rotation at which the wing has finished rotation at the end of each half stroke produces maximum lift (mean C_L=1.74). **b** Symmetrical rotation (mean C_L=1.67) and **c** delayed rotation at which the wing rotates at the beginning of the half stroke. Delayed rotation produces approximately 70% less lift (mean C_L=1.01) than advanced wing rotation. *Black arrows* on the fly body indicate magnitude and orientation of the mean flight force vector and *coloured sections* of the wing tip path indicate the phase of wing rotation

rotational axis at which a wing is not producing any circulation while rotating can be as low as 0.57 (Sane and Dickinson 2002). This observation might have direct consequences for the evolution of wing shape design because it favours wings with a rotational axis close to the leading edge (Walker 2002a). If the position of the rotational axis falls behind the critical distance of 0.57 or 0.75 the wing even produces negative circulation which subtracts from translational circulation and lowers the production of aerodynamic lift (Fig. 4c). Wings in which $\hat{x}_0$ is small should be thus beneficial for an insect that produces rotational circulation at the stroke reversals. However, the benefit of rotational circulation for flight force enhancement does not depend solely on the geometric wing axes but also on the *timing* of wing rotation within the stroke cycle.

The reason that the contribution of rotational circulation may change is that the wing is translating while it rotates (Fig. 4; Dickinson et al. 1999). A kinematic pattern in which the wing is starting and finishing its rotation before it reverses the direction at the end of the down-stroke is termed *advanced rotation* and the wing's rotational axis appears to be located near the leading edge of the wing (Fig. 4a). This type of stroke reversal adds rotational circulation to translational circulation that results in a pronounced lift peak at the end of each half stroke (Fig. 5a, red trace). Alternatively, the wing may rotate at the beginning of the next following half stroke (up-stroke in Fig. 4b). This is termed *delayed rotation* and the true rotational axis lies near the trailing wing edge. Because of the opposite sign between rotational and translational circulation, this kinematic manoeuvre subtracts lift from translational lift, which results in negative lift peaks (Fig. 5c, red trace). Although there is only a small difference in rotational timing (8%) between both cases, flight force production is 1.7 times higher during advanced rotation when using a generic kinematic pattern of wing motion.

In insects that show rather symmetrical rotational motion, such as *Drosophila* (Lehmann 1994; Zanker 1990a), the process of rotation spans the end of one half stroke to the beginning of the next, then the wing produces first an upward force (positive lift) and then, following stroke reversal, a downward force (negative lift). Remarkably, the overall benefit of the symmetrical rotation is only several percentage points less compared with an advanced wing rotation offering an insect a larger safety margin for flight control when altering rotational

timing during steering manoeuvres (±70 μs in *Drosophila*; Dickinson et al. 1993). The potential benefit of rotational circulation for a flying insect is quite remarkable. The robotic model wing yields that rotational effects may contribute between 35% (fruit fly kinematics) and 50% (hover fly kinematics) to total lift production averaged throughout the stroke cycle – a high value considering the brief duration over which they act in flapping wing motion (Dickinson et al. 1999).

The Kramer effect

A third method, besides that of rotational and Magnus circulation, of how wing rotation may contribute to total lift production in flapping insect wings is its ability to delay stall during wing translation. Although, in the hawkmoth and the fruit fly, leading-edge vorticity appears to be stable throughout the translational phase of wing motion, the delay of stall might be beneficial in insects flying at high Reynolds number and elevated forward speed. Kramer (1932) has demonstrated that a wing in steady motion may experience lift coefficients above the steady stall value when the wing is rotating with a low rotational spin from low to high angles of attack. The increase in maximum lift coefficient is termed the Kramer effect, which is not due to the induced rotational circulation, which can be shown by estimating rotational forces from Eq. 14 (Ellington 1984d; Munk 1925). In turn, a wing stalls at smaller angle of attack when it rotates with a negative rotational velocity in which the angle of attack is steadily decreasing (Farren 1935). In generic kinematic patterns used for modelling insect flight, the latter situation is given when wing rotation is delayed during the stroke reversals, which might explain some of the lift attenuation measured in the physical fruit fly model (Dickinson et al. 1999; van den Berg and Ellington 1997; Wang 2000a). In contrast, when the wing rotates in advance, the angle of attack is steadily increasing, which might facilitate leading-edge vortex stability due to the Kramer effect. In sum, whether the Kramer effect is of functional significance for flapping insect wings still remains unclear and further analytical modelling and experiments seem to be required to answer this question in all details.

Wake–wing interference: wake capture

In contrast to the wings of an aeroplane that typically moves through still air, the wings of helicopters, wind turbines and hovering insects intercept with the wake created by the wing's own motion. The most prominent example of wake–wing interaction is induced flow and its possible role in stabilising leading-edge vorticity as mentioned above. Besides this important finding, physical wing models have revealed that wake–wing interaction at the stroke reversals might significantly contribute to lift production in hovering insects (Dickinson et al. 1999). Although vorticity shed into wake is the primary cause for this lift enhancement, the underlying fluid mechanical mechanism does not rely on Kutta circulation. Dickinson et al. (1999) termed this mechanism *wake capture* that is thought to produce aerodynamic lift by a transfer of fluid momentum to the wing at the beginning of each half stroke.

The wake capture mechanism was discovered by dissecting the measured force traces in the robotic *Drosophila* wing (Fig. 5). Although rotational circulation can explain one of the stroke reversal forces, it cannot explain a large positive transient lift peak that develops immediately after the wing changes the direction of motion. This force peak is distinct from rotational lift because its timing is independent of the phase of wing rotation. The transient lift enhancement even persists when the wing is halted after wing rotation, indicating that the wake produced by the wing motion in the previous half stroke serves as an energy source for lift production. Superficially it sounds paradoxical that a wing can regain lift from fluid motion created in a previous half stroke. However, wakes are a manifestation of energy lost to the external medium by a moving object and part of this energy could potentially be extracted from the wake. The energy seen in the wake resides as kinetic energy in the motion of the fluid that the wing accelerated during motion.

According to the momentum theory of insect flight, lift production of a flapping insect wing depends on the change in air momentum per unit time (Ellington 1984d). The kinetic energy that appears in the momentum jet, however, can be quite different because kinetic energy E_{kin} is the product of the mass of the accelerated fluid volume and speed squared given by

$$E_{kin} = \frac{1}{2} m u_i^2 \tag{15}$$

The energy spent in order to generate a certain air momentum is less and flight is more efficient when the flapping wings accelerate a large amount of air at low velocity rather than a small fluid volume at high speed. Although both cases may produce the same fluid momentum rate, and thus similar lift, the kinetic energy of the moving fluid differs (Ellington 1984d). In flight an insect may adjust fluid speed and the amount of accelerated air mass by changing the ratio between stroke frequency and stroke amplitude (Alexander 1982; Götz 1968, 1983; Heide 1971; Lehmann and Dickinson 1998, 2001; Zanker 1990b). The extraction of kinetic energy from the wake behind a flying insect might have been demonstrated recently in freely flying butterflies during take-off in which smoke trails have been used to visualise the flow around the moving wings (Srygley and Thomas 2002). The images suggest that at the beginning of the upstroke the volume of the shed stopping vortex increases, while its vorticity decreases after the wing has intercepted with the wake. When a wing extracts kinetic energy from the wake there is a transfer of fluid momentum on the

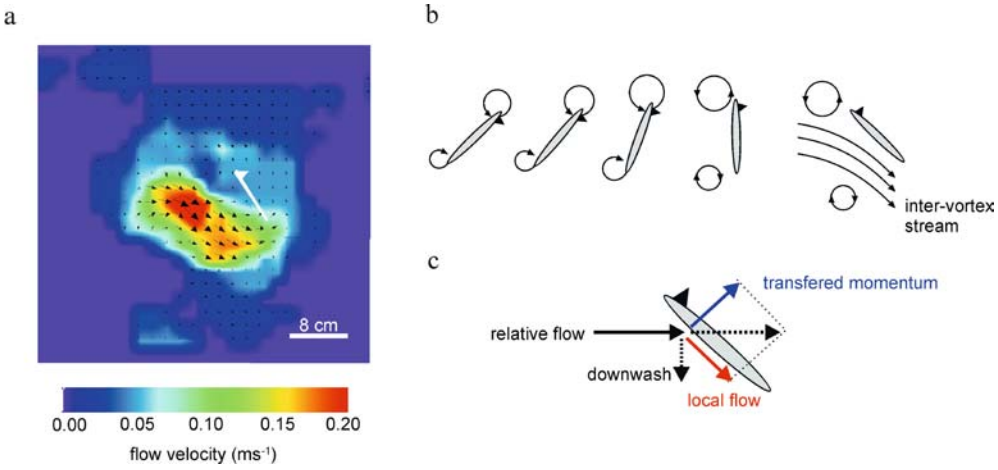

Fig. 6a–c Momentum transfer due to the wake capture mechanism at stroke reversal in a robotic *Drosophila* wing. **a** Flow through the mid-chord of the wing (*white bar*, *triangle* indicates leading edge of dorsal wing surface) immediately before a complete stop. *Arrow* length and direction indicate magnitude and orientation of the local fluid velocities. Fluid velocity is also indicated by *pseudo-colour coding*. The flow image was taken using particle-image-velocimetry (PIV). A more detailed description of the method is found in Dickinson et al. (1999). **b** Schematic of wake capture mechanism during advanced wing rotation. Leading- and trailing-edge vortices that are generated during wing translation and rotation are shed into the wake at the end of each half stroke. The vortex system generates an inter-vortex stream towards the wing. **c** Momentum transfer during wake capture. The wing deflects the oncoming fluid (*solid black arrow*) downwards (*red arrow*). The change in fluid direction and velocity indicates that a fluid momentum (*blue*) is transferred to the wing which may generate lift at the beginning of each half stroke. In a *Drosophila* kinematic wing pattern, wake capture forces may explain approximately 23% of total lift production

wing that in turn enhances lift production and thus increases total flight efficiency (Fig. 6c).

Detailed investigations on robotic wings have drawn a more comprehensive and mechanistic picture of wing–wake interaction (Dickinson et al. 1999). Based on a generic stroke kinematics, the force traces show that even small modifications in wing motion significantly alter the benefit of wake capture for aerodynamic lift production (Figs. 5 and 6). Both the magnitude of momentum transfer and its contribution to lift critically depend on the timing of wing rotation, which is quite similar to the mechanisms that determine rotational circulation (Dickinson et al. 1999). The model wing only produces positive wake capture lift when wing rotation precedes stroke reversal and the flow intercepts with the wing at a positive angle of attack (Figs. 5a and 6).

When wing rotation is delayed with respect to the stroke reversal, the angle of attack is negative with respect to the oncoming flow and thus lift is negative (Fig. 5c). With symmetrical rotation, the wing has a 90° angle of attack at the midpoint of the stroke reversal, lift is negligible whereas drag is high (Fig. 5b). These results show that independent of rotational timing the transfer of momentum seems to occur immediately after the wing has changed its direction of motion. Whether or not wake capture forces are beneficial for lift production in turn depends on rotational timing, which determines the wing's angle of attack at the moment of the energy recovery. Maximum forces were measured during an advanced rotation when strong leading- and trailing-edge vorticity is shed into the wake (Fig. 6b). The analysis of PIV images suggests that the opposite spin of both vortices produces an *inter-vortex stream* that is directed towards the wing surface. As more circulation is produced by the wing at the end of the half stroke, so more vorticity can be shed and the inter-vortex stream becomes stronger. Alterations in fluid velocity within the inter-vortex flow might explain why during advanced rotation wake capture force peaks are large and positive; small and positive during symmetrical wing rotation and small and negative if rotation is delayed (Fig. 5).

Although the magnitude of force production following a prominent rotational effect underscores the remarkable significance of the wake capture concept for flight force enhancement in hovering flight, the contribution of wake capture force might be limited to low advance ratios. Fast forward flight stretches out the wake in space and wing–wake interaction (wake capture) is thought to become reduced. Nevertheless even if wake capture forces are negligible in fast forward flight, their importance lies in the fact that they enhance lift production during the most demanding form of flight – that is, hovering flight – in which all lift has be to produced by the wing's own flapping motion.

Added mass effects and analytical models

The interpretation of wake capture force generation given above has been questioned recently by the use of computational fluid dynamics (CFD) modelling of flapping insect wings, suggesting that the rotational-independent lift peak is due to a reaction of accelerating an added mass of fluid and does not rely on a momentum transfer

of the fluid (Sun and Tang 2002). In the past the effect of inertial reaction forces during the stroke reversals has been well recognised and discussed as a cause for wing rotation, twisting and bending (Daniel and Combes 2002; Ennos 1988a). For example, in two species of flies, the blowfly *Calliphora vicina* and the hoverfly *Eristalis tenax*, the high stroke frequency ranging from 100 to 200 Hz produces inertial forces that are sufficiently high to elicit passive wing pitch (angle of attack) changes when the wing reverses its direction of motion (Ennos 1988b). Moreover, the high compliance of the wing base makes it unlikely that wing pitch changes during rotation are caused by active rotation at the wing articulation in these two fly species (Ennos 1988b).

In general, acceleration forces could play a significant role in the aerodynamics of insect flight (Osborne 1951). When a wing accelerates within a fluid it must set the surrounding air in motion, thus facing inertial forces by the fluid that is accelerated. The inertia of the flapping wing is increased by the mass of the accelerated fluid termed added mass or virtual mass (Katz and Plotkin 2002). Unfortunately, the evaluation of virtual mass, and thus an estimation of inertial forces, is not always easy because in most situations the local fluid acceleration may be caused by effects other than the wing's motion, such as the time-dependent wake-induced downwash. Although the mass of a wing itself could be tiny, the mass of the accelerated fluid might not be (Ellington 1984a, 1984c; Lehmann and Dickinson 1997). Particularly in dynamically scaled physical wing models in which air is replaced by mineral oil, the added mass might be quite high. Thus, when the wing accelerated at the beginning of each half stroke, added mass might produce considerable inertial forces similar to wake capture force. Sane and Dickinson (2001) presented an estimate of inertial forces for the robotic *Drosophila* wing and stated that added mass might contribute only a little to total lift during the stroke reversals. Nevertheless, total force balance in flapping flight must not only consider circulatory forces produced during wing translation (Kutta circulation and LEV), wing rotation (rotational and Magnus circulation, and Kramer effect), circulation due to dorsal wing interaction between the left and the right wing (*clap and fling*, see below), but also wake capture forces and inertial forces due to the acceleration of fluid mass.

It is difficult to determine exactly the contribution of wing inertia in physical model wings because of the uncertainties in estimating added mass. However, this problem can be circumvented by solving the Navier-Stokes equation for the fluid motion around the wing using CFD modelling. Once the wake has been calculated from wing kinematics, lift and drag forces can be derived from the mathematical model and compared with the measured forces of the physical model (Sun and Tang 2002). The outcome of the CFD study is surprising because it shows that, even when the vorticity of the LEV is shed from the previous half stroke, the lift coefficient does not increase at the beginning of the next following stroke but slightly decreases instead. The two free vortices shed at the end of each half produce a downwash that *decreases* the effective angle of attack of the wing and thus lowers lift production instead of producing extra lift via momentum transfer. The wake capture peak then would be a result of the acceleration force when the real and virtual (added mass) wing mass accelerates at the beginning of the following half stroke (Sun and Tang 2002). The detrimental interpretation of CFD-modelled wake on one side and wake and force reconstructed from physical wing models on the other side clearly demonstrates the complexity of unsteady force production in insects and that more studies are required to understand fully the basis of flight force production in flapping flight.

The example above has shown that analytical models of virtual flapping wings may greatly contribute to our understanding of how flapping wings produce lift using aerodynamic theory. Besides modelling the flow around the wing using CFD, other mathematical models use an unsteady blade element concept to derive unsteady forces from flapping wing motion. Over the last decade computational modelling regarding insect flight has been done using potential flow models for the fruit fly (Ramamurti and Sandberg 2001; Walker 2002b), a moth (Smith 1996) and other forms of flapping flight (DeLaurier 1993; Kamakoti et al. 2000; Liu 2002; Vest and Katz 1996; Zbikowski 2002). The benefit of analytical models lies in their capability to predict and verify experimental results on robotic wings which allows aerodynamicists to approach insect flight aerodynamics from two different perspectives.

Wing–wing interference: the clap and fling mechanism

One of the most complex kinematic manoeuvres described in flying animals is the physical interaction of the left and right beating wing during the dorsal stroke reversal termed the 'clap and fling'. This was found in tiny wasps (Weis-Fogh 1973, 1975), various Diptera (Ellington 1984c; Ennos 1989), lacewings (Antonova et al. 1981), damselfly (Wakeling and Ellington 1997a) and a whitefly (Wootton and Newman 1979). A modified kinematics termed the 'clap and peel' was found in fixed flying *Drosophila* (Götz 1987) and larger insects such as butterflies (Brackenbury 1991a; Brodsky 1991), bush cricket, mantis (Brackenbury 1990, 1991b) and locust (Cooter and Baker 1977). Although the clap and fling might not be used continuously during flight, several insect species use this behaviour during maximum locomotor performance while carrying loads (Marden 1987) or performing power-demanding flight turns (Cooter and Baker 1977). Marden's experiments on various insect species have shown that insects with clap and fling wing beat produce about 25% more aerodynamic lift per unit flight muscle (79.2 N kg^{-1} mean value) than insects using conventional wing kinematics (some fly species, bugs, mantids, dragonflies, bees, wasps, beetles, sphinx moths; 59.4 N kg^{-1} mean value).

The clap and fling is a close apposition of two wings at dorsal stroke reversal preceding pronation that is thought to strengthen the development of circulation during the down-stroke (Weis-Fogh 1973). The fling phase preceding the down-stroke is thought to enhance circulation due to fluid inhalation in the cleft formed by the moving wings causing strong vortex generation at the leading edge while the development of trailing-edge vorticity is partly inhibited by trailing-edge wing contact. The development of leading-edge vorticity does not violate Kelvin's law of angular momentum conservation because the net circulation of the LEVs in the two wings amounts to zero due to their opposite rotational spin. Despite the lack of direct evidence, studies in the past have emphasised that clap and fling might augment unsteady aerodynamic forces in flapping flight based on kinematic patterns of the small wasp *Encarsia formosa*. However, these studies solely estimated the benefit of the fling part of wing motion using either two-dimensional analytical models (Edwards and Cheng 1982; Ellington 1975; Lighthill 1973) or a combined approach incorporating measurements of flow velocities (Bennett 1977; Maxworthy 1979) and forces (Spedding and Maxworthy 1986; Sunada et al. 1993) in simple robotic wings, but ignored any aerodynamic alterations due to the clap part of wing motion at the end of the up-stroke, including wake history. The overall benefit of the clap and fling thus remains uncertain in many studies of insect wing kinematics as well its robustness against changes in the angular distance between both wings (near clap condition) during dorsal wing excursion or changes in stroke shape.

According to Weis-Fogh (1974), the magnitude of LEV circulation developed during the fling phase can be expressed as

$$\Gamma_f = \omega c^2 g(a) \tag{16}$$

in which ω is the rate of change of angle of attack in each wing and $g(a)$ is a function of the angle of leading edge wedge opening prior to trailing-edge motion. For a robotic wing travelling 6 chord widths at high Reynolds number of 83,000, Bennett (1977) estimated the potential gain in total lift due to the clap and fling to be 15%. He also conjectured that no significant lift enhancement by the fling manoeuvre will be apparent in the case of small insects flying at intermediate and low Reynolds numbers (Bennett 1977). However, in experiments using the three-dimensional robotic *Drosophila* wings travelling 3–4 chord widths we found a similar value for lift gain (12–15%), although in these experiments Reynolds number was relatively small (50–200) and the wings did not physically touch (*near-fling*, F.-O. Lehmann et al., unpublished data). Our data also show that the benefit of the clap and fling depends on the angular separation between both wings and may vanish when the wings are separated by more than 10° stroke amplitude. As well as the benefit for enhancing total flight forces, the high force peaks during the fling phase might be beneficial in controlling nose-down pitching moments by displacing the centre of lift in a rearward position, which is comparable to tilting the wing tip plane in helicopters by increasing lift developed by the rearmost blade (Bennett 1977).

Conclusions and future directions

Within the last few years considerable progress has been made in the identification of unsteady state aerodynamic mechanisms and their contribution to lift production in flapping insect flight. Physical robotic wings have proven aerodynamic concepts that have been predicted for several decades and experimental results have been used to refine analytical non-steady aerodynamic modelling, such as non-steady elementary blade concepts and computational fluid dynamics. Computer models add valuable knowledge to the overall picture of insect flight because they may predict aerodynamic forces and flow structures under various fluid dynamic conditions and different stroke kinematics. However, the complexity of flow structures produced when an insect is moving freely in the air will still be a challenge for analytical modelling and thus ongoing experimental research will be necessary. Moreover, the repertoire of non-steady-state aerodynamic mechanisms that an insect may use to produce and enhance lift is remarkable and the contribution of each single mechanism is assumed to vary between different insect species (Dickinson et al. 1999; Srygley and Thomas 2002). Moreover, the recent experimental and analytical results show that even subtle changes in stroke kinematics might change lift production tremendously in a flying insect. Thus, in order to present a more comprehensive theory of flight that evaluates unsteady aerodynamic mechanisms with respect to their importance for lift enhancement, flight efficiency, and flight control appears to be one of the major goals in the future (Taylor 2001).

After decades of research on tethered flying animals, extended investigations on freely flying insects will complement and refine the biological concepts of flapping flight which have been constructed in the past. The current results derived from model wings, moreover, may lead into new research activities on the neuromuscular system of insects, including a more comprehensive description of flight energetics. For this reason, an integrative approach in which behavioural studies, robotics and analytical models are combined might enable researchers to evaluate in greater detail the process of how fluid dynamic constraints have shaped the neuromuscular system of a flying insect. Eventually, modern three-dimensional high-speed video techniques for evaluating manoeuvrability in freely flying insects combined with three-dimensional imaging techniques such as particle-image-velocimetry to quantify the flow around an insect's wing and body in space, should help us to understand more of the complexity of one of the most demanding forms of locomotion that has been evolved in the animal kingdom.

References

Alexander DE (1982) Studies on flight control and aerodynamics in dragonflies. PhD dissertation, Duke University, N.C.

Alexander DE (1986) Wind tunnel studies of turns by flying dragonflies. J Exp Biol 122:81–98

Antonova OA, Brodsky AK, Ivanov VD (1981) Wing beat kinematics of five insect species. Zool Zh 60:506–518

Azuma A, Watanabe T (1988) Flight performance of a dragonfly. J Exp Biol 137:221–252

Bennett L (1966) Insect aerodynamics: vertical sustaining force in nectar-hovering flight. Science 152:1263–1266

Bennett L (1970) Insect flight: lift and rate of change of incidence. Science 167:177–179

Bennett L (1977) Clap and fling aerodynamics: an experimental evaluation. J Exp Biol 69:261–272

Berg C van den, Ellington CP (1997) The three-dimensional leading-edge vortex of 'hovering' model hawkmoth. Philos Trans R Soc Lond B 352:329–340

Birch JM, Dickinson MH (2001) Spanwise flow and the attachment of the leading-edge vortex on insect wings. Nature 412:729–733

Brackenbury J (1990) Wing movements in the bush cricket *Tettigonia viridissima* and the mantis *Ameles spallanziana* during natural leaping. J Zool 220:593–602

Brackenbury J (1991a) Kinematics of take-off and climbing flight in butterflies. J Zool 224

Brackenbury J (1991b) Wing kinematics during natural leaping in the mantids *Mantis religiosa* and *Iris oratoria*. J Zool 223:341–356

Bradley RG, Smith CW, Wray WO (1974) An experimental investigation of leading-edge vortex augmentation by blowing. NASA

Brodsky AK (1991) Vortex formation in the tethered flight of the peacock butterfly *Inachis io* L. (Lepidoptera, Nymphalidae) and some aspects of insect flight evolution. J Exp Biol 161:77–95

Brodsky AK (1994) The evolution of insect flight. Oxford University Press, New York

Buckholz RH (1981) Measurements of unsteady periodic forces generated by the blowfly flying in a wind tunnel. J Exp Biol 90:163–173

Campbell JF (1976) Augmentation of vortex lift by spanwise blowing. J Aircraft 13:727–732

Chadwick LE (1940) The wing motion of the dragonfly. Bull Brooklyn Entomol Soc 35:109–112

Chaplygin SA (1956) The selected works on wing theory of Sergei A. Chaplygin. San Francisco

Cooter RJ, Baker PS (1977) Weis-Fogh clap and fling mechanism in *Locusta*. Nature 269:53–54

Crompton B, Thomason JC, McLachlan A (2003) Mating in a viscous universe: the race is to the agile, not to the swift. Proc R Soc Lond B 270:1991–1995

Daniel TL, Combes SA (2002) Flexible wings and fins: bending by inertial or fluid-dynamic forces? Integr Comp Biol 42:1044–1049

David CT (1978) The relationship between body angle and flight speed in free flying *Drosophila*. Physiol Entomol 3:191–195

De Vries O (1983) On the theory of the horizontal-axis wind turbine. Annu Rev Fluid Mech 15:77–96

DeLaurier JD (1993) An aerodynamic model for flapping-wing flight. Aeronaut J 1993:125–130

Dickinson MH (1996) Unsteady mechanisms of force generation in aquatic and aerial locomotion. Am Zool 36:537–554

Dickinson MH, Lehmann F-O, Götz KG (1993) The active control of wing rotation by *Drosophila*. J Exp Biol 182:173–189

Dickinson MH (1994) The effects of wing rotation on unsteady aerodynamic performance at low Reynolds numbers. J Exp Biol 192:179–206

Dickinson MH, Götz KG (1993) Unsteady aerodynamic performance of model wings at low Reynolds numbers. J Exp Biol 174:45–64

Dickinson MH, Götz KG (1996) The wake dynamics and flight forces of the fruit fly, *Drosophila melanogaster*. J Exp Biol 199:2085–2104

Dickinson MH, Lehmann F-O, Sane S (1999) Wing rotation and the aerodynamic basis of insect flight. Science 284:1954–1960

Dixon CJ, Theisen JG, Scuggs RM (1973) Theoretical and experimental investigations of vortex-lift control by spanwise blowing. Experimental Research 1: LG73ER-0169

Dudley R (2002) Mechanisms and implications of animal flight maneuverability. Integr Comp Biol 42:135–140

Dudley R, Ellington CP (1990a) Mechanics of forward flight in bumblebees. I. Kinematics and morphology. J Exp Biol 148:19–52

Dudley R, Ellington CP (1990b) Mechanics of forward flight in bumblebees. II. Quasi-steady lift and power requirements. J Exp Biol 148:53–88

Edwards RH, Cheng HK (1982) The separation vortex in the Weis-Fogh circulation-generation mechanism. J Fluid Mech 120:463–473

Egelhaaf M (1989) Visual afferences to flight steering muscles controlling optomotor responses of the fly. J Comp Physiol A 165:719–730

Ellington CP (1975) Non-steady-state aerodynamics of the flight of *Encarsia formosa*. In: Wu TY (ed) Symposium on swimming and flying in nature 2. Proceedings of the second half of the symposium on swimming and flying in nature. Pasadena, Calif., pp 729–762

Ellington CP (1980) Vortices and hovering flight. In: Nachtigall W (ed) Instationäre Effekte an schwingenden Flügeln. Steiner, Wiesbaden, pp 64–101

Ellington CP (1984a) The aerodynamics of insect flight. II. Morphological parameters. Philos Trans R Soc Lond B 305: 17–40

Ellington CP (1984b) The aerodynamics of insect flight. III. Kinematics. Philos Trans R Soc Lond B 305:41–78

Ellington CP (1984c) The aerodynamics of insect flight. IV. Aerodynamic mechanisms. Philos Trans R Soc Lond B 305:79–113

Ellington CP (1984d) The aerodynamics of insect flight. V. A vortex theory. Philos Trans R Soc Lond B 305:115–144

Ellington CP (1984e) The aerodynamics of hovering insect flight. I. The quasi-steady analysis. Philos Trans R Soc Lond B 305:1–15

Ellington CP (1999) The novel aerodynamics of insect flight: applications to micro-air vehicles. J Exp Biol 202:3439–3448

Ellington CP, Berg C van den, Willmott AP, Thomas ALR (1996) Leading-edge vortices in insect flight. Nature 384:626–630

Ennos AR (1988a) The importance of torsion in the design of insect wings. J Exp Biol 140:137–160

Ennos AR (1988b) The inertial cause of wing rotation in Diptera. J Exp Biol 140:161–169

Ennos AR (1989) The kinematics and aerodynamics of the free flight of some Diptera. J Exp Biol 142:49–85

Farren WS (1935) The reaction on a wing whose angle of incidence is changing rapidly. Rep Memo Aeronaut Res Commun 1561

Flick KC, Tu MS, Daniel TL (2001) Flight control by steering muscles in *Manduca sexta*. Am Zool 41:1445

Fry SN, Sayaman R, Dickinson MH (2003) The aerodynamics of free-flight maneuvers in *Drosophila*. Science 300:495–498

Fung YC (1993) An introduction to the theory of aeroelasticity. Dover, New York

Gleason M, Roskam J (1972) Preliminary results of some experiments with a vortex augmented wing. In: National Business Aircraft meeting, SAE 720321. Wichita, Kans.

Götz KG (1968) Flight control in *Drosophila* by visual perception of motion. Biol Cybernetics 4:199–208

Götz KG (1983) Bewegungssehen and Flugsteuerung bei der Fliege *Drosophila*. In: Nachtigall W (ed) BIONA report 2. Fischer, Stuttgart, pp 21–34

Götz KG (1987) Course-control, metabolism and wing interference during ultralong tethered flight in *Drosophila melanogaster*. J Exp Biol 128:35–46

Götz KG, Hengstenberg B, Biesinger R (1979) Optomotor control of wing beat and body posture in *Drosophila*. Biol Cybernetics 35:101–112

Grodnitsky DL, Morozov PP (1993) Vortex formation during tethered flight of functionally and morphologically two-winged insects, including evolutionary considerations on insect flight. J Exp Biol 182:11–40

Ham ND, Garelick MS (1968) Dynamic stall considerations in helicopter rotors. J Am Helicopter Soc 13:49–55

Hausen K, Wehrhahn C (1990) Neural circuits mediating visual flight control in flies. II. Separation of two control systems by microsurgical brain lesions. J Neurosci 10:351–360

Heide G (1971) Die Funktion der nicht-fibrillären Flugmuskeln bei der Schmeißfliege *Calliphora*. II. Muskuläre Mechanismen der Flugssteuerung und ihre nervöse Kontrolle. Zool Jb Physiol 76:99–137

Heide G (1975) Properties of a motor output system involved in the optomotor response in flies. Biol Cybernetics 20:99–112

Heide G (1983) Neural mechanisms of flight control in Diptera In: Nachtigall W (ed) BIONA report 2. Fischer, Stuttgart, pp 35–52

Heide G, Götz KG (1996) Optomotor control of course and altitude in *Drosophila* is achieved by at least three pairs of flight steering muscles. J Exp Biol 199:1711–1726

Heisenberg M, Wolf R (1988) Reafferent control of optomotor yaw torque in *Drosophila melanogaster*. J Comp Physiol A 163:373–388

Heisenberg M, Wolf R (1993) The sensory-motor link in motion-dependent flight control of flies In: Miles FA, Wallman J (eds) Visual motion and its role in the stabilization of gaze. Elsevier, Amsterdam, pp 265–283

Hoff W (1919) Der Flug der Insekten und Vögel. Naturwissenschaften 10:159–162

Hollick FSJ (1940) The flight of the dipterous fly *Muscina sabulans* Fallén. Philos Trans R Soc Lond B 230:357–390

Holst E von, Küchemann D (1941) Biologische und aerodynamische Probleme des Tierflugs. Naturwissenschaften 29:348–362

Houghton EL, Carpenter PW (2003) Aerodynamics for engineering students. Butterworth-Heinemann, Oxford

Ivanov VD (1990) A comparative analysis of flight aerodynamics of caddis flies (Insecta: Trichoptera). Zool Zh 69:46–60

Jensen M (1956) Biology and physics of locust flight. III. The aerodynamics of locust flight. Philos Trans R Soc Lond B 239:511–552

Kamakoti R, Berg M, Ljungqvist D, Shyy W (2000) A computational study for biological flapping wing flight. Trans Aeronaut Astronaut Soc Rep China 32:265–279

Kamakoti R, Lian Y, Regisford S, Kurdila A, Shyy W (2002) Computational aeroelasticity using a pressure-based solver. CMES 3:773–789

Katz J, Plotkin A (2002) Low-speed aerodynamics. Cambridge University Press, Cambridge

Kliss M, Somps C, Luttges MW (1989) Stable vortex structures: a flat plate model of dragonfly hovering. J Theor Biol 136:209–228

Kokshaysky NV (1979) Tracing the wake of a flying bird. Nature 279:146–148

Krall KM, Haight CH (1972) Wind tunnel tests of a trapped vortex-high lift airfoil. Advanced Technology Center, USA

Kramer M (1932) Die Zunahme des Maximalauftriebes von Tragflügeln bei plötzlicher Anstellwinkelvergrösserung (Böeneffect). Z Flugtech Motorluftschiff 82:223–240

Kruppa EW (1977) A wind tunnel investigation of the Kasper vortex concept. Paper 115704, American Institute of Aeronautics and Astronautics (AIAA), Washington, D.C.

Kuethe AM, Chow C-Y (1986) Foundations of aerodynamics. Wiley, New York

Lan CE (1979) The unsteady quasi-vortex-lattice method with applications to animal propulsion. J Fluid Mech 93:747–765

Land MF, Collett TS (1974) Chasing behaviour of houseflies (*Fannia canicularis*). J Comp Physiol A 89:331–357

Lehmann F-O (1994) Aerodynamische, kinematische und electrophysiologische Aspekte der Flugkrafterzeugung und Flugkraftsteuerung bei der Taufliege *Drosophila melanogaster*. Thesis, Max-Planck-Institute for Biological Cybernetics, University of Tübingen, Germany

Lehmann F-O (2000) Flattern für Flugkräfte. Naturwiss Rundschau 623:223–230

Lehmann F-O, Dickinson MH (1997) The changes in power requirements and muscle efficiency during elevated force production in the fruit fly, *Drosophila melanogaster*. J Exp Biol 200:1133–1143

Lehmann F-O, Dickinson MH (1998) The control of wing kinematics and flight forces in fruit flies (*Drosophila* spp.). J Exp Biol 201:385–401

Lehmann F-O, Dickinson MH (2001) The production of elevated flight force compromises flight stability in the fruit fly *Drosophila*. J Exp Biol 204:627–635

Lighthill MJ (1973) On the Weis-Fogh mechanism of lift generation. J Fluid Mech 60:1–17

Liu H (2002) Computational biological fluid dynamics: digitizing and visualizing animal swimming and flying. Integr Comp Biol 42:1050–1059

Liu H, Ellington CP, Kawachi K, Berg C van den, Willmott AP (1998) A computational fluid dynamic study of hawkmoth hovering. J Exp Biol 201:461–477

Marden J (1987) Maximum lift production during take-off in flying animals. J Exp Biol 130:235–258

Maxworthy T (1979) Experiments on the Weis-Fogh mechanism of lift generation by insects in hovering flight. 1. Dynamics of the 'fling'. J Fluid Mech 93:47–63

McCroskey WJ, Carr LW, McAlister KW (1976) Dynamic stall experiments on oscillating airfoils. AIAA J 14:57–63

Milne-Thomson LM (1966) Theoretical aerodynamics. Macmillan, New York

Mises R von (1959) Theory of flight. Dover, New York

Munk MM (1925) Note on the air forces on a wing caused by pitching. NACA Tech Notes 217:1–6

Nachtigall W (1977) Die aerodynamische Polare des Tipula-Flügels und eine Einrichtung zur halbautomatischen Polarenaufbahme. In: Nachtigall W (ed) Physiology of movement: biomechanics. Fischer, Stuttgart, pp 347–352

Nachtigall W (1979) Rasche Richtungsänderungen und Torsionen schwingender Fliegenflügel und Hypothesen über zugeordnete instationäre Strömungseffekte. J Comp Physiol A 133:351–355

Newman BG, Savage SB, Schouella D (1977) Model tests on a wing section of an *Aeschna* dragonfly scale effects in animal locomotion. In: Pedley TJ (ed) Scale effects in animal locomotion. Academic Press, London, pp 445–477

Norberg RA (1975a) Hovering flight of the dragonfly *Aeschna juncea* L. In: Wu TY, Brokaw CJ, Brennen C (eds) Kinematics and aerodynamics, vol 2. Plenum, New York, pp 763–781

Norberg UM (1975b) Hovering flight in the pied flycatcher (*Ficedula hypoleuca*). In: Wu TY, Brokaw CJ, Bremen C (eds) Swimming and flying in nature, vol 2. Plenum, New York, pp 869–881

Norberg UM (1976) Aerodynamics of hovering flight in the long-eared bat *Plecotus auritus*. J Exp Biol 28:221–245

Norberg UML (2002) Structure, form, and function of flight in engineering and the living world. J Morphol 252:52–81

Okamoto M, Yasuda K, Azuma A (1996) Aerodynamic characteristics of the wings and body of a dragonfly. J Exp Biol 199:281–294

Osborne MFM (1951) Aerodynamics of flapping flight with application to insects. J Exp Biol 28:221–245

Polhamus EC (1971) Predictions of vortex-lift characteristics by a leading-edge suction analogy. J Aircraft 8:193–199

Ramamurti R, Sandberg WC (2001) Computational study of 3-D flapping foil flows. Paper AIAA 2001-0605, AIAA, Washington, D.C.

Rayner JMV (1979) A vortex theory of animal flight. 1. The vortex wake of a hovering animal. J Fluid Mech 91:697–730

Rayner JMV, Jones G, Thomas A (1986) Vortex flow visualizations reveal change in upstroke function with flight speed in bats. Nature 321:162–164

Reavis MA, Luttges MW (1988) Aerodynamic forces produced by a dragonfly. AIAA paper 88-0330, AIAA, Washington, D.C.
Rossow VJ (1978) Lift enhancement by an externally trapped vortex. J Aircraft 15:618–625
Saharon D, Luttges MW (1987) Three-dimensional flow produced by a pitching-plunging model dragonfly wing. AIAA paper 87-0121, AIAA, Washington, D.C.
Sane S, Dickinson M (2001) The control of flight force by a flapping wing: lift and drag production. J Exp Biol 204:2607–2626
Sane SP, Dickinson MH (2002) The aerodynamic effects of wing rotation and a revised quasi-steady model of flapping flight. J Exp Biol 205:1087–1096
Savage SB, Newman BG, Wong DT-M (1979) The role of vortices and unsteady effects during the hovering flight of dragonflies. J Exp Biol 83:59–77
Schenato L, Deng X, Sastry S (2001) Flight control system for a micromechanical flying insect: architecture and implementation. In: IEEE international conference on robotics and automation, Seoul, Korea
Schlichting H (1979) Boundary-layer theory. McGraw-Hill, New York
Shyy W, Berg M, Ljungqvist D (1999) Flapping and flexible wings for biological and micro air vehicles. Prog Aeronaut Sci 35:455–505
Silcox RJ, Szware WJ (1974) Wind-tunnel dynamic analysis of an oscillating airfoil. AIAA paper 74-259, AIAA, Washington D.C.
Smith MJC (1996) Simulating moth wing aerodynamics: towards the development of flapping-wing technology. AIAA J 34: 1348–1355
Spedding GR (1986) The wake of a jackdaw (*Corvus mondela*) in slow flight. J Exp Biol 125:287–307
Spedding GR, Maxworthy T (1986) The generation of circulation and lift in a rigid two-dimensional fling. J Fluid Mech 165:247–272
Spedding GR, Rayner JMV, Pennycuick CJ (1984) Momentum and energy in the wake of a pigeon (*Columba livia*) in slow flight. J Exp Biol 111:81–102
Srygley RB, Dudley R (1993) Correlations of the position of center of body mass with butterfly escape tactics. J Exp Biol 174:155–166
Srygley RB, Thomas ALR (2002) Unconventional lift-generating mechanisms in free-flying butterflies. Nature 420:660–6604
Stepniewski WZ, Keys CN (1984) Rotary-wing aerodynamics. Dover, New York
Sun M, Hamdani H (2001) A study on the mechanism of high-lift generation by an airfoil in unsteady motion at low Reynolds Number. Acta Mech Sin (Eng Ser) 17:97–114
Sun M, Tang J (2002) Lift and power requirements of hovering flight in *Drosophila virilis*. J Exp Biol 205:2413–2427
Sunada S (1993) Fundamental analysis of three-dimensional 'near fling'. J Exp Biol 183:217–248
Sunada S, Kawachi K, Watanabe I, Azuma A (1993) Fundamental analysis of three-dimensional "near fling". J Exp Biol 183:217–248
Sunada S, Takashima H, Hattori T, Yasuda K, Kawachi K (2002) Fluid-dynamic characteristics of a bristled wing. J Exp Biol:2737–2744
Taylor GK (2001) Mechanics and aerodynamics of insect flight control. Biol Rev 76:449–471
Thom A, Swart P (1940) The forces on an aerofoil at very low speeds. J R Aeronaut Soc 44:761–770
Tu MS, Dickinson MH (1996) The control of wing kinematics by two steering muscles of the blowfly, *Calliphora vicina*. J Comp Physiol A 178:813–830
Usherwood JR, Ellington CP (2002a) The aerodynamic of revolving wings. I. Model hawkmoth wings. J Exp Biol 205:1547–1564
Usherwood JR, Ellington CP (2002b) The aerodynamics of revolving wings. II. Propeller force coefficients from mayfly to quail. J Exp Biol 205:1565–1576
Vest MS, Katz J (1996) Unsteady aerodynamic model of flapping wings. AIAA J 34:1435–1440
Vogel S (1967a) Flight in *Drosophila*. II. Variations in stroke parameters and wing contour. J Exp Biol 46:383–392
Vogel S (1967b) Flight in *Drosophila*. III. Aerodynamic characteristics of fly wings and wing models. J Exp Biol 46:431–443
Vogel S (1994) Life in moving fluids. Princeton University Press, Princeton, N.J.
Wagner H (1925) Über die Entstehung des dynamischen Auftriebes von Tragflügeln. Z Angew Math Mech 5:17–35
Wagner H (1985) Aspects of the free flight behaviour of houseflies (*Musca domestica*). In: Gewecke M, Wendler G (eds) Insect locomotion. Parey, Hamburg, pp 223–232
Wakeling JM, Ellington CP (1997a) Dragonfly flight. II. Velocities, accelerations, and kinematics of flapping flight. J Exp Biol 200:557–582
Wakeling JM, Ellington CP (1997b) Dragonfly flight. III. Lift and power requirements. J Exp Biol 200:583–600
Walker GT (1925) The flapping flight of birds. J R Aeronaut Soc 29:590–594
Walker JA (2002a) Functional morphology and virtual models: physical constraints on the design of oscillating wings, fins, legs and feet at intermediate Reynolds numbers. Integr Comp Biol 42:232–242
Walker JA (2002b) Rotational lift: something different or more of the same? J Exp Biol 205:3783–3792
Walker JA, Westneat MW (2000) Mechanical performance of aquatic rowing and flying. Proc R Soc Lond B 267:1875–1881
Wang H, Zeng L, Liu H, Chunyong Y (2003) Measuring wing kinematics, flight trajectory and body attitude during forward flight and turning maneuvers in dragonflies. J Exp Biol 206:745–757
Wang ZJ (2000a) Two dimensional mechanism for insect hovering. Phys Rev Lett 85:2216–2219
Wang ZJ (2000b) Vortex shedding and frequency selection in flapping flight. J Fluid Mech 410:323–341
Wang ZJ, Birch JM, Dickinson MH (2003) Unsteady forces and flows in low Reynolds number hovering flight: two-dimensional computation vs robotic wing experiments. J Exp Biol 207:449–460
Wehrhahn C, Poggio T, Bülthoff H (1982) Tracking and chasing in house flies (*Musca*): an analysis of 3-D flight trajectories. Biol Cybernetics 45:123–130
Weis-Fogh T (1956) Biology and physics of locust flight. II. Flight performance of the desert locust (*Schistocera gregaria*). Philos Trans R Soc Lond B 239:459–510
Weis-Fogh T (1972) Energetics of hovering flight in hummingbirds and in *Drosophila*. J Exp Biol 56:79–104
Weis-Fogh T (1973) Quick estimates of flight fitness in hovering animals, including novel mechanisms for lift production. J Exp Biol 59:169–230
Weis-Fogh T (1974) In: Wu TY, Brokaw CJ, Brennen C (eds) Swimming and flying in nature, vol 2. Plenum, New York, pp 729–762
Weis-Fogh T (1975) Unusual mechanisms for the generation of lift in flying animals. Sci Am 233:80–87
Willmott AP (1995) The mechanics of hawkmoth flight. Thesis, Cambridge University, Cambridge
Willmott AP, Ellington CP (1997a) Measuring the angle of attack of beating insect wings: robust three-dimensional reconstruction from two-dimensional images. J Exp Biol 200:2693–2704
Willmott AP, Ellington CP (1997b) The mechanics of flight in the hawkmoth *Manduca sexta*. I. Kinematics of hovering and forward flight. J Exp Biol 200:2705–2722
Willmott AP, Ellington CP, Thomas ALR (1997) Flow visualization and unsteady aerodynamic mechanisms in the flight of the hawkmoth *Manduca sexta*. Philos Trans R Soc Lond B 352:303–316
Wootton RJ, Newman DJS (1979) Whitefly have the highest contradiction frequencies yet recorded in non-fibrillar flight muscles. Nature 280:402–403

Wu JZ, Vakili AD, Wu JM (1991) Review of the physics of enhancing vortex lift by unsteady excitation. Prog Aerospace Sci 28:73–131

Zanker JM (1990a) The wing beat of *Drosophila melanogaster*. I. Kinematics. Philos Trans R Soc Lond B 327:1–18

Zanker JM (1990b) The wing beat of *Drosophila melanogaster*. III. Control. Philos Trans R Soc Lond B 327:45–64

Zanker JM, Götz KG (1990) The wing beat of *Drosophila melanogaster*. II. Dynamics. Philos Trans R Soc Lond B 327:19–44

Zbikowski R (2002) On aerodynamic modeling of an insect-like flapping wing in hover for micro air vehicles. Philos Trans R Soc Lond A 360:273–290

Zeil J (1983) Sexual dimorphism in the visual system of flies: the free flight behavior of male Bibionidae (Diptera). J Comp Physiol A 150:395–412